

The

GERMAN MOUSE CLINIC

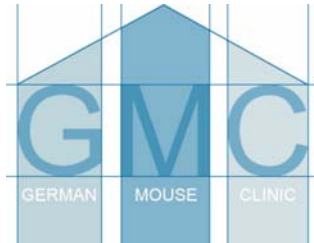
at the Helmholtz Zentrum München
German Research Center for
Environmental Health (GmbH)

Report for HST012

Confidential Data

Helmut Fuchs, Valérie Gailus-Durner, Christoph Lengger, Beatrix Naton, Thure Adler, Juan Antonio Aguilar Pimentel, Lore Becker, Ines Bolle, Julia Calzada-Wack, Claudia Dalke, Nicole Ehrhardt, Barbara Ferwagner, Lillian Garrett, Wolfgang Hans, Sabine M. Hölder, Gabriele Hölzlwimmer, Marion Horsch, Anahita Javaheri, Magdalena Kallnik, Eva Kling, Holger Maier, Ilona Moßbrugger, Cornelia Prehn, Ildikó Rácz, Birgit Rathkolb, Jan Rozman, Regine Schreiner, Anja Schrewe, Ralf Steinkamp, Monja Willershäuser, Jurek Adamski, Johannes Beckers, Heidrun Behrendt, Dirk H. Busch, Irene Esposito, Jack Favor, Jochen Graw, Gerhard Heldmaier, Heinz Höfler, Boris Ivandic, Hugo Katus, Martin Klingenspor, Thomas Klopstock, Martin Mempel, Markus Ollert, Leticia Quintanilla-Martinez, Jörg Schmidt, Holger Schulz, Eckhard Wolf, Wolfgang Wurst, Andreas Zimmer, and Martin Hrabé de Angelis

The German Mouse Clinic



The German Mouse Clinic (GMC) was founded January 2002 at the Helmholtz Zentrum München - German Research Center for Environmental Health (GmbH) in Munich to provide an open access platform for standardized mouse phenotyping. The GMC is supported by the National Genome Research Network (NGFN, <http://www.ngfn.de/>) and is a partner of the EUMORPHIA research program (<http://www.eumorphia.org/>).

In the GMC, experts from various fields of mouse genetics, physiology and pathology in close collaboration with clinicians work side by side at one location. We offer a primary phenotypic analysis of mouse mutants (more than 320 parameters) in the areas of allergology, behavior, bone and cartilage, cardiovascular diseases, clinical chemistry, energy metabolism, eye development and vision, immunology, lung function, molecular phenotyping, neurology, nociception, pathology, and steroid metabolism. Additional screens for host-pathogen interaction can be performed at the HZI Braunschweig. Secondary and tertiary screening for in-depth analysis is offered by the different screens and is available on request.

Director

Prof. Dr. Martin Hrabé de Angelis
Institute of Experimental Genetics
Helmholtz Zentrum München
German Research Center for
Environmental Health (GmbH)
Ingolstädter Landstraße 1
D-85764 Neuherberg / München
Tel.: 089-3187-3302
Fax: 089-3187-3500

HelmholtzZentrum münchen
German Research Center for Environmental Health



Content

1	Summary.....	1
1.1	Primary Screening	1
2	General Part.....	3
2.1	Generation of the Mutant Mouse Line and Known Phenotypes	3
2.2	The Role of the Gene.....	3
2.3	Expected Phenotypes	3
2.4	Suggested Human Disease Model.....	4
2.5	Mice	4
2.5.1	Number and kind of mice	4
2.5.2	Housing conditions	4
2.6	Workflow	5
2.6.1	Standardized workflow for the primary screen in the German Mouse Clinic.....	5
2.6.2	Applied screens	6
2.6.3	Quality Assurance.....	6
2.7	Statistical Analysis of Data.....	8
2.8	References.....	8
3	Specific part	10
3.1	Dysmorphology, Bone and Cartilage	10
3.1.1	Introduction	10
3.1.2	Summary	10
3.1.3	Mice	10
3.1.4	Material and Methods	11
3.1.5	Results and Discussion.....	13
3.1.6	References	13
3.2	Behavior Screen	22
3.2.1	Introduction	22
3.2.2	Summary	22
3.2.3	Mice	22
3.2.4	Material and Methods	22
3.2.5	Results.....	23
3.2.6	Discussion	23
3.2.7	References	23
3.3	Metabolic Screen	25
3.3.1	Introduction	25
3.3.2	Summary	25
3.3.3	Mice	25
3.3.4	Material and Methods	25
3.3.5	Parameters	26
3.3.6	Results and Discussion.....	26
3.3.7	Suggestions for Secondary Screening.....	27
3.3.8	References	27
3.4	Clinical Chemistry and Hematology	29
3.4.1	Introduction	29
3.4.2	Summary	29
3.4.3	Mice	29

3.4.4	Materials and Methods.....	29
3.4.5	Parameters	31
3.4.6	Results.....	32
3.4.7	Discussion	33
3.4.8	Recommendations for Secondary Screening.....	34
3.4.9	References	34
3.5	Immunology Screen	46
3.5.1	Introduction	46
3.5.2	Summary	46
3.5.3	Mice	46
3.5.4	Material and Methods	46
3.5.5	Parameters	47
3.5.6	Results and Discussion.....	48
3.5.7	References	48
3.6	Allergy Screen.....	54
3.6.1	Introduction	54
3.6.2	Summary	54
3.6.3	Mice	54
3.6.4	Material and Methods	54
3.6.5	Results and Discussion.....	55
3.6.6	References	55
3.7	Steroid Metabolism Screen	58
3.7.1	Introduction	58
3.7.2	Summary	58
3.7.3	Mice	58
3.7.4	Material and Methods	58
3.7.5	Results and Discussion.....	59
3.7.6	References	60
3.8	Molecular Phenotyping	61
3.8.1	Introduction	61
3.8.2	Summary	61
3.8.3	Methods and Materials.....	61
3.8.4	Results.....	63
3.8.5	Discussion	67
3.8.6	References	69

1 Summary

1.1 Primary Screening

In a customized screen 60 mice (20 homozygous mutant, 20 heterozygous mutant, and 20 wild-type control littermates) of the HST012 mutant mouse line have been analyzed in the German Mouse Clinic (GMC) in the screens Dysmorphology, Behavior, Energy Metabolism, Clinical Chemistry, Immunology, Allergy, Steroid Metabolism, Cardiovascular Function, Molecular Phenotyping, and Pathology. The screens Neurology, Eye, Nociception, Pathology, and Lung Function have been omitted. The screening started on May 5th, 2007. The results are briefly summarized below by screen.

Dysmorphology, Bone and Cartilage: DXA and pQCT analyses revealed that the HST012 mutant mouse line showed an osteopenic phenotype. In addition, increased plasma calcium and alkaline phosphatase (ALP) activity measured by the clinical-chemical screen might suggest a higher bone turnover and/or a defect in bone mineralization in homozygous mutants.

Energy Metabolism: Body mass and body temperature were reduced in mutant mice. Metabolic rate was decreased in mutants as expected for lower body mass but food intake was significantly increased. Interestingly, this was a gradual effect most evident in homozygous mutants. No significant effect of the mutation on metabolic fuel utilization could be detected.

Clinical Chemistry and Hematology: Besides the previously known phenotype of impaired kidney function, indicated by increased urea and creatinine values, we detected reduced blood lipid values indicating an influence on energy metabolism, and increased ALP activity and calcium concentrations that might be due to changes in bone metabolism. Blood gas analysis, hematology and iron metabolism-related parameters revealed subtle changes that might be due to secondary effects or simply findings by chance due to biological variation.

Immunology: A statistically higher expression of CD62L within the CD8 cell cluster occurred in female mutants. In male mutant mice, the proportion of Ly6C expressing cells within the CD8+ T-cell cluster was decreased, in females a higher proportion of Ly6C, CD44 co-expressing CD8 T-cells was found. The analysis of the blood plasma showed slightly higher levels of IgG2a antibodies in female HST012 mutant mice.

Molecular Phenotyping: The data analysis and various statistical methods detected several genes differentially regulated between mutant and reference tissue. Several of the significantly regulated genes in *kidney* are annotated with hemolytic anemia, glomerulosclerosis, hypertension, diabetes and tumorigenesis

In the screens **Behavior**, **Allergy**, and **Steroid Metabolism**, no genotype-specific differences could be found.

The screens **Neurology**, **Eye**, **Nociception**, **Lung Function**, and **Pathology** have been cancelled.

Cardiovascular: Data from the cardio-vascular screening will be submitted later.

Please contact Valérie Gailus-Durner to discuss further steps and details.

2 General Part

2.1 Generation of the Mutant Mouse Line and Known Phenotypes

The mouse line HST012 was established in the recessive clinical-chemical screen of the Munich ENU-Mouse-Mutagenesis-Project hosted at the Helmholtz Zentrum München at the beginning of 2004. The founder animal had been selected for inheritance testing due to a reproducibly increased urea concentration in plasma. The mutation was mapped to the distal part of chromosome 7 and candidate gene sequencing revealed a point mutation in the uromodulin gene (aa substitution A227T).

The mutant mice show the following alterations:

- increase of urea, uric acid and potassium in plasma,
- slightly increased daily urinary excretion and moderate defective urinary concentration ability,
- immunohistochemical and electron microscopic alterations of thick ascending limb cells of Henle's loop,
- slightly reduced body weight.

All further findings which will be shown in this report we consider as new.

2.2 The Role of the Gene

The uromodulin gene encodes for the uromodulin glycoprotein, also called the Tamm-Horsfall (THP), which is the most abundant urinary protein in mammals. THP may be involved in the pathogenesis of cast nephropathy, urolithiasis, and tubulointerstitial nephritis. In addition, analyses with THP-knockout mice revealed a protective effect of THP against ascending urinary tract infection. THP may also play a regulatory role in the kidney.

2.3 Expected Phenotypes

The provider expects any phenotype connected to altered kidney function, e.g., alterations in blood electrolyte and blood gas parameters as well as blood pressure. Several secondary effects are possible like altered bone metabolism, chronic inflammation of the gastrointestinal system. It is known from human patients that uremia causes apathy and drowsiness by toxic effects on the central nervous system.

2.4 Suggested Human Disease Model

Possible are Familial juvenile hyperuricemic nephropathia (FJHN), Medullary cystic kidney disease type 2 (MCKD 2), and Dominant glomerulocystic kidney disease (GCKD; please see OMIM data base entry # [*191845](#)).

2.5 Mice

2.5.1 Number and kind of mice

Table 1: HST012 mice provided for analysis.	
Genotype / Sex	Number of Animals
Homozygous mutant female	10
Homozygous mutant male	10
Heterozygous mutant female	10
Heterozygous mutant mal	10
Control female	10
Control male	10

As described by the sender, the mice analyzed were a 5th generation back-cross to C3HeB/FeJ wild type.

2.5.2 Housing conditions

In the GMC mice are housed in type II polycarbonate cages in individually ventilated caging (IVC) systems (VentiRack Bioscreen TM, Biozone, Margate, UK) on wood fiber (Altromin, Lage, Germany). The IVCs operate with positive pressure. Mice are transferred in weekly intervals to new cages with forceps in Laminar Flow Class II changing stations. Mice are fed with irradiated standard rodent high energy breeding diet (Altromin 1314) and given semidemineralized filtered (0.2 µm) water *ad libitum*. Light is adjusted to a 12h/12h light/dark cycle; temperature and relative humidity are regulated to 22 ± 1°C and 55 ± 5%, respectively. In specified modules husbandry conditions are adjusted according to the experiment requirements (See corresponding sections). All people attending the facility completely change their garment (jackets and trousers autoclaved) and shoes and wear caps and masks before entering the GMC (Brielmeier *et al.*, 2002).

Outbred 8-week-old male SPF Swiss mice are used as sentinels and kept on a mixture of new bedding and aliquots of soiled bedding (50:50) from all cages of the IVC rack. In addition, the sentinels were also exposed to soiled air from all “upstream” cages of the IVC rack. Health monitoring is carried out by on-site examination of the sentinel mice by certified laboratories according to FELASA recommendations (www.felasa.org).

Mice are kept according to the German laws. Tests were carried out by authority of the Regierung von Oberbayern.

2.6 Workflow

2.6.1 Standardized workflow for the primary screen in the German Mouse Clinic

Mouse mutants entering the GMC are examined in a primary screen according to the following standard workflow (Fig. 1; modified after Gailus-Durner, Fuchs *et al.*, 2005; Brown *et al.*, 2005). Analyzed parameters are listed in Table 2. After the mice arrive at the GMC, they are acclimatized in the new environment for four weeks and divided into two groups to enter the GMC in two pipelines (Fig. 1).

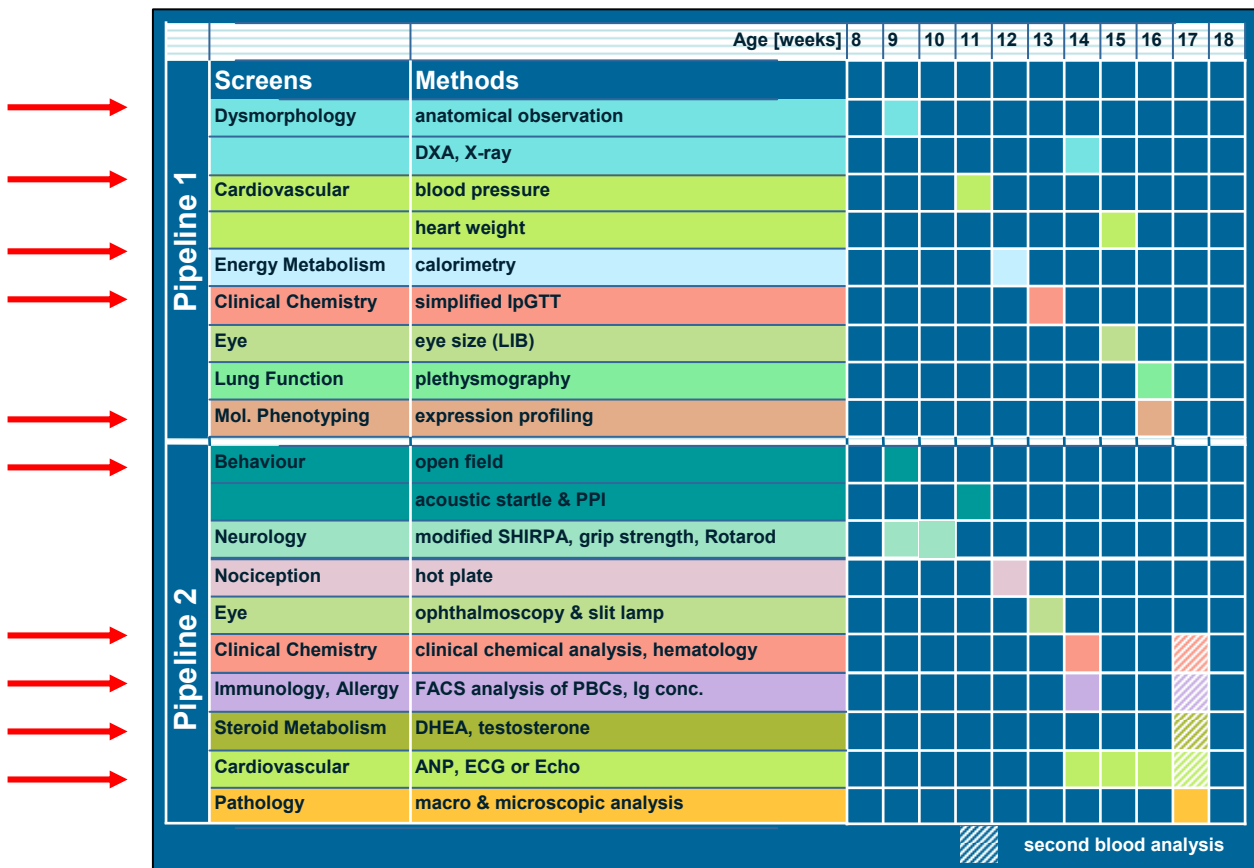


Figure 1: Workflow of the primary screen

Explanation below, ▨ Analysis of blood-based parameters.

The mice of the **first pipeline** are subjected to a morphological whole-body checkup in the Dymorphology Screen and are passed to the Cardiovascular Screen. After the blood pressure is taken, the energy metabolism is analyzed

by calorimetry. One week later a simplified IpGTT is performed by the Clinical Chemical Screen. In the next week, the mice re-enter the Dysmorphology Screen for X-ray and DXA analysis. After the determination of eye size parameters, 12 mutant animals (six males / six females) and 12 controls (six males / six females) leave the animal facility for the Lung Function Analysis, which for technical reasons is located elsewhere. The males are used to freeze organs for future molecular phenotyping on request.

The **second pipeline** starts in the Behavior Screen. The initial screening of the naïve mice includes also neurological tests and lasts three weeks. One week later, the animals are tested in the Nociceptive Screen. On the following week the mice go through the tests of the Eye Screen. When the mice are 14 weeks old, blood is taken, and samples are distributed to the blood-based screens for Clinical Chemistry, Immunology, Cardiovascular, and Allergy. One week later the mice were passed to the Cardiovascular Screen wherein the mice stay two weeks. ANP level is determined in the plasma samples, whereas ECG or Echo analysis is performed on request. Three weeks after testing of the first blood sample, a second sample is taken to confirm the findings and analyze steroid levels. After completion of the primary screen all animals of the second pipeline are analyzed macro- and microscopically in the Pathology.

Deviations from our Standard operation procedure (SOP) are listed below; please take the specific number of analyzed animals from the sections of the applied screen.

2.6.2 Applied screens

The GMC standard workflow for the primary screen as described above was applied to analyze the HST012 mice. As the demanded number of 120 animals (20 mice per sex per genotype of homozygous, heterozygous and control animals) could not be delivered, the workflow was adapted to the available number of animals. The Dysmorphology Screen performed secondary screening (pQCT). The screens Neurology, Eye, Nociception, Pathology, and Lung Function have been omitted.

2.6.3 Quality Assurance

The Quality Assurance as part of the Quality Management at the GMC consists of the following elements: standardized analyses via Standard Operating Procedures (SOP) and validation of analysis protocols by different institutions within the EUMORPHIA program, standardized data and project management supported by the central database system MausDB (Maier *et al.*, 2008) and the GMC coordination tool CoordDB as well as Quality Control and continuous training of the staff.

Coordination of the GMC's operations

The GMC management team (Core Facility) coordinates the scientific issues, logistics and administration of the GMC. The coordination software tool Co-ordDB supports the GMC management team in handling the incoming phenotyping requests and managing the complex phenotyping workflow of the primary and secondary screening. Besides the operational business activities the management team organizes the expansion of the screening services in collaboration with its partners. Additionally, the management arranges regular training of the staff members and the clinic's quality assurance.

Standardized Operation Procedures (SOP) and Validation of Protocols

The GMC developed a set of SOPs which cover all steps from mouse import and handling to phenotyping and data analysis. These SOPs are strictly followed during the whole screening process in the GMC and all procedures are documented.

The GMC is one of the major partners of the EUMODIC consortium that emerged from the EUMORPHIA program (Brown *et al.*, 2005), a consortium for the selection, establishment, and standardization of phenotyping protocols for mice as models for human diseases and for mouse husbandry. Cross-validation of protocols by EUMORPHIA is performed by the different institutions. A collection of the protocols (EMPreSS) is posted on the EUMORPHIA web site at (<http://www.eumorphia.org/EMPreSS/>; Mallon *et al.*, 2008).

Central Database System

Another tool for quality assessment is the central database system which ensures full traceability of samples and documentation of all data. All mouse data is entered into the system (e.g. date of birth, sex, cage) and all screening results linked to the corresponding SOP as well as any changes of the mouse conditions are immediately put in.

Quality Control

In addition to routinely screen-specific quality control tests, control animals of selected strains (e.g. C57BL/6 and C3HeB/FeJ) are analyzed through the standard protocol for all phenotypes at regular intervals. This data is reviewed by the coordination team.

A tissue archive has been established for the storage of tail and blood plasma samples taken from all mice that have ever been analyzed in the GMC. The tail clips can be used for post-hoc genotyping in case of doubtful genotype information. The sanitary status of every mouse completing the screening can be tested by means of these plasma samples.

Continuous Training

Regularly specific training courses are held at the GMC. Specialists are invited to give lectures and to offer practical training at special days. Staff training is documented and maintained by the management team.

2.7 Statistical Analysis of Data

If not otherwise stated, data was analyzed by ANOVA or Student's t-test (In the t-test, data of males and females was analyzed separately). Tables summarizing the data will show mean \pm standard error of the mean. Significant differences are indicated stepwise from 0.05, 0.02, 0.01, 0.001 to 0.0001. Raw data are available in Excel sheets on request.

2.8 References

Brielmeier M., H. Fuchs, G. Przemec, V. Gailus-Durner, M. Hrabé de Angelis, and J. Schmidt (2002): The GSF-Phenotype Analysis Center (German Mouse Clinic, GMC): A sentinel-based health-monitoring concept in a multi-user unit for standardized characterization of mouse mutants. In: J.-L. Guenet and C. Herweg (eds.) *Laboratory Animals Science - Basis and Strategy for Animal Experimentation* Vol. 11, Proceedings of the 8th FELASA Symposium, Laboratory Animals Ltd., Aachen, pp. 19-22.

Brown SD, Chambon P, Hrabé de Angelis M; Eumorphia Consortium. (2005): EMPReSS: standardized phenotype screens for functional annotation of the mouse genome. *Nat Genet.* 37(11): 1155

Gailus-Durner, V., Fuchs, H. *et al.* (2005): Introducing the German Mouse Clinic: open access platform for standardized phenotyping. *Nature Methods* 2: 403 - 404.

Maier H, Lengger Ch, Simic B, Fuchs H, Gailus-Durner V, Hrabé de Angelis M (2008): MausDB: an open source application for phenotype data and mouse colony management in large-scale mouse phenotyping projects. *BMC Bioinformatics* 9: 169 (Epub 26 March 2008)

Mallon AM, Blake A, Hancock JM. (2008): EuroPhenome and EMPReSS: online mouse phenotyping resource. *Nucleic Acids Res.* 2008 Jan; 36 (Database issue):D715-8. Epub 2007 Sep

Abbreviations and Wording

HST012	Mutant mouse line displaying altered Harnstoff (urea) levels
THP	Tamm-Horsfall glycoprotein, also known as uromodulin
GMC	German Mouse Clinic
IVC	individually ventilated cage
control	homozygous wild-type control, <i>HST012</i> ^{+/+}
het	heterozygous mutant, <i>HST012</i> ^{+/-}
hom	homozygous mutant, mutant <i>HST012</i> ^{-/-}
wt	wild type
FELASA	Federation of E uropean L aboratory A nimal S cience A ssociations, 25 Shaftesbury Avenue, London W1D 7EG, UK, www.felasa.org

Table 2: Primary Screen at GMC		
Screens	Goal	Methods
Dysmorphology, Bone and Cartilage	morphological analysis of body, skeleton, bone, and cartilage	morphological observation, bone densitometry, X-ray
Behavior	locomotion and anxiety-related behavior sensory motor gaiting	open field Acoustic startle & PPI
Neurology	assessment of muscle, spinocerebellar, sensory, and autonomic function	modified SHIRPA protocol grip strength Rotarod
Eye	assessment of morphological alterations of the eye	funduscopy laser interference biometry slit lamp biomicroscopy
Nociception	detection of altered pain response	hot plate assay
Energy Metabolism	measurement of body weight, body temperature, activity, O ₂ consumption, CO ₂ production, respiratory exchange ratio	indirect calorimetry
Clinical Chemistry and Hematology	determination of clinical-chemical and hematological parameters in blood glucose tolerance	blood autoanalyzer, ABC-animal blood counter simplified IpGTT
Steroid Metabolism	analysis of steroid hormones in blood plasma: testosterone and DHEA	ELISA
Immunology	analysis of peripheral blood samples for immunological parameters	flow cytometry, Multiplex Bead Array
Allergy	analysis of total plasma IgE	ELISA
Cardiovascular	assessment of functional cardio-vascular parameters analysis of plasma ANP	non-invasive tail-cuff blood pressure measurement, surface limb ECG / Echo, heart weight, ELISA
Lung Function	assessment of alterations in breathing patterns	whole body plethysmography (Buxco [®])
Molecular Phenotyping	RNA expression profiling	DNA-chip technology
Pathology	microscopic and macroscopic examination	histology, immunochemistry

3 Specific part

3.1 Dysmorphology, Bone and Cartilage

3.1.1 Introduction

In the Dysmorphology, Bone and Cartilage Screen of the German Mouse Clinic mice are analyzed for morphological abnormalities in different organ systems with special focus on bone and cartilage development and homeostasis. The aim of the screen is to establish mouse models for human skeletal diseases like osteoporosis (McLean & Olsen, 2001; Rosen *et al.*, 2001), scoliosis (Giampietro *et al.*, 2003), limb defects (Mariani & Martin, 2003), osteogenesis imperfecta (Rauch & Glorieux, 2004; Chipman *et al.*, 1993) or osteoarthritis (Abe *et al.*, 2006). We adapted the successful dysmorphological screening protocol from the Munich ENU-Mutagenesis Screen (Hrabé de Angelis *et al.* 2000) for use in the German Mouse Clinic. The nomenclature of the parameters was adapted according to the Mammalian Phenotype Ontology wording (www.informatics.jax.org/searches/MP_form.shtml). Further tests for defects in bone development and homeostasis were taken over from human diagnosis, and were adapted for the use in mice analysis. Such tests include: X-ray analysis, bone densitometry, and, in special cases, micro computed tomography. Detailed protocols for screening for bone and cartilage phenotypes in mice are described in Fuchs *et al.* (2006).

3.1.2 Summary

In the morphological investigation via visual inspection and X-ray analysis, no genotype-specific differences were found. In the dual-energy X-ray absorptiometry (DXA), we observed significant differences in bone and body parameters between mutants and controls.

To further analyze the observed differences in the bone parameters, we performed a secondary screen by pQCT analysis at the age of 6 month. In the femoral bone metaphysis and diaphysis, total and cortical bone content, and cortical bone area were significantly reduced in homozygous male mutants (same tendency in females for total and cortical bone content) compared to wild-type mice. Additionally total, trabecular and cortical bone density were significantly decreased at the femoral diaphysis in male homozygous mutants (same tendency in females) compared to wild-type mice.

In summary DXA and pQCT analyses revealed that the HST012 mutant mouse line showed an osteopenic phenotype. In addition, increased serum calcium and alkaline phosphatase (ALP) activity measured by the clinical-chemical screen might suggest a higher bone turnover and/or a defect in bone mineralization in homozygous mutants.

3.1.3 Mice

Thirty male (10 +/+, 10 +/-, 10 -/-) and 30 female (10 +/+, 10 +/-, 10 -/-) mice were analyzed by morphological inspection at the age of 10-12 weeks. 15-17-week-old mutants (17 +/-, 14 -/- and 17 +/-, 15 -/- animals for DXA and X-ray

analysis, respectively) and controls (16 animals) entered the bone density and X-ray analysis. Six-month-old mutants (20 +/-, 19 -/-) and controls (21 animals) entered the pQCT analysis.

3.1.4 Material and Methods

The Dysmorphology, Bone and Cartilage module of the German Mouse Clinic analyzed the mice in different phases:

1. At the age of five weeks, i.e. when the mice entered the facility, the general physical condition and health were checked,
2. at the age of nine weeks, a morphological observation as a whole-body checkup was performed; and
3. at the age of 14 weeks, X-ray analysis and bone densitometry were performed.

Morphological Observation

The animals were screened using the protocol for morphological analysis from Fuchs *et al.* (2000) as adapted for the German Mouse Clinic.

Using a clickbox (supplied by the MRC Institute of Hearing Research, Nottingham, UK) we tested the mice's ability to hear a sound of 20 kHz. The reaction of the animals was classified into six categories (0=no reaction at all, 1=no Preyer reflex, 2= retarded reaction, 3= normal reaction, 4= strong reaction, 5= particularly strong reaction).

X-ray Images

Equipment: Faxitron X-ray Model MX-20 (Specimen Radiography System, Illinois, USA),

NTB Digital X-ray Scanner EZ 40 (NTB GmbH, Diepholz, Germany),

Quality control: Calibration of the system is done in monthly intervals,

Settings: Voltage 25 kV, integration time 40 ms,

Procedure: The anesthetized mouse was fixed on an X-ray-permeable plate and placed in the machine. Using iX-Pect software supplied by the manufacturer of the X-ray scanner, the image was taken and analyzed. Analysis was done qualitatively by visual inspection of the images as well as quantitatively by using the ruler tool of iX-Pect software.

Bone density analysis

Equipment: pDEXA Sabre X-ray Bone Densitometer (Norland Medical Systems. Inc., Basingstoke, Hampshire, UK; distributed by Stratec Medizintechnik GmbH, Pforzheim, Germany),

Quality control: Calibration of the system was done in daily intervals using the QC and the QA phantoms delivered by the manufacturer. Results from the quality control were recorded by the system.

Settings: Scan speed 20 mm/s, Resolution 0.5 mm x 1.0 mm, HAW 0.020

Procedure: After anesthesia, the weight and length of the mouse were recorded, and the mouse was placed in the analyzer. After a scout scan, the area of interest was optimized and the measure scan started.

Data-analysis: For analysis of the data, regions have to be defined. The standard analysis comprises a whole body analysis as well as a whole body analysis excluding the skull.

pQCT (peripheral quantitative computed tomography) analysis

Equipment: Stratec XCT Research SA+ (Stratec Medizintechnik GmbH, Pforzheim, Germany). Photons emitted by the X-ray tube are detected by 12 semiconductor detectors. The spatial resolution was set to 70 μm .

Quality control: Routine calibration of the system was performed daily with a phantom sample provided by the manufacturer. Results from the quality control were recorded by the system.

Settings: Translation-rotation scanner, scan speed max. 40 mm/s, resolution 70-500 μm . Research M mode (collimator position B; green; 0.25 x 0.9 mm).

Procedure: After anesthesia, the weight and length of the mouse were recorded. The mouse leg was positioned with a plastic holder in the centre of the gantry opening and fixed with a plastic clip. We examined the distal femoral metaphysis and diaphysis of the left femur from each mouse to obtain volumetric bone mineral density, content and area of the trabecular, cortical, and total bone. Once the scout view was completed, the reference line for the CT scans was set at the most distal point of the femur (knee joint space). At 3.0 mm proximal from the reference line, two slices were taken at 0.25 mm intervals and at 6.0 mm proximal from the reference line one slice was taken to give characteristic cross sections of the femoral metaphysis and diaphysis, respectively.

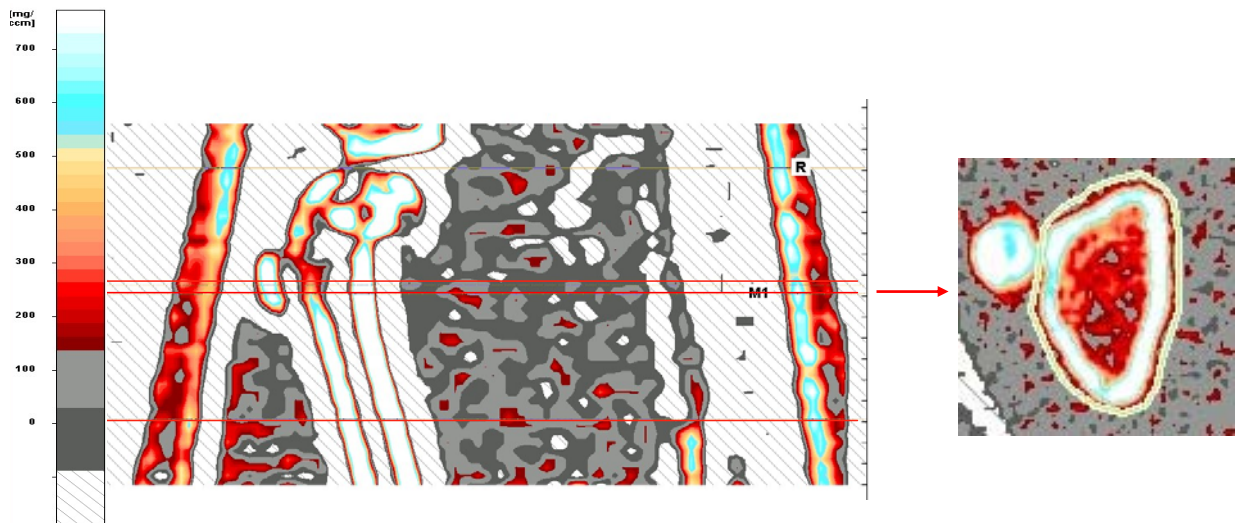


Figure 2: pQCT scout view and CT scan of the femur.

After the scout view (left picture) a reference line (R) for the CT scans (right picture) was set. Two CT slices (red lines) were taken in the femoral metaphysis and one in the diaphysis.

Data-analysis: After scanning, regions of interest were defined by separating the femur from the patella. The CT slices were analyzed using contour mode 1, cortmode 1 and peelmode 2 to evaluate trabecular and cortical parameters. For detection of the outer contour of bone a threshold was set at 350 mg/cm^3

and the trabecular bone region was defined by setting an inner threshold to 450 mg/cm³.

Statistical analysis of data

Analysis of quantitative data sets was carried out using SigmaStat (Systat Software, Inc.) and StatView software package (SAS corporation).

3.1.5 Results and Discussion

Sixty animals of HST012 mutant mouse line were analyzed in the Dymorphology, Bone and Cartilage module of the German Mouse Clinic. In the morphological investigation via visual inspection and X-ray analysis, no genotype-specific differences were found (Tables 3 and 4). In the Clickbox test (Table 5) to test the hearing ability of the mice, we observed a normal reaction in mutants and controls. In the bone densitometry using DXA analysis (Table 6), we detected significantly reduced BMD and BMC, but significantly increased sBMD (only homozygous; BMD related to the body weight) values in heterozygous and homozygous mutants compared to controls. Body weight, body length (only homozygous), fat mass and fat content were significantly decreased, lean content was significantly increased in heterozygous and homozygous mutants compared to controls. The sex differences we observed are common in many mouse strains, and thus are not abnormal (unpublished data).

To further analyze the observed differences in the bone parameters, we performed a **secondary screen** by pQCT analysis. pQCT technology enables real volumetric bone density measurements in g/cm³ and it separates cortical and trabecular bone compartments and thus can monitor metabolic changes very quickly and precisely (Gasser, 2003; Schmidt *et al.*, 2003). For *in vivo* monitoring of bone density, mass and architecture, pQCT analysis is restricted to locations of the appendicular skeleton and tail vertebra.

In the femoral bone metaphysis and diaphysis, total and cortical bone content, and cortical bone area were significantly reduced in homozygous male mutants (same tendency in females for total and cortical bone content) compared to wild-type mice (Table 7 and 8). Additionally total, trabecular and cortical bone density were significantly decreased at the femoral diaphysis in male homozygous mutants (same tendency in females) compared to wild-type mice (Table 8).

In summary, DXA and pQCT analyses revealed that the HST012 mutant mouse line showed an **osteopenic** phenotype. In addition, increased serum calcium and alkaline phosphatase (ALP) activity measured by the clinical-chemical screen might suggest a **higher bone turnover** and/or a **defect in bone mineralization** in homozygous mutants.

3.1.6 References

Abe K., Fuchs H., Lisse T., Hans W. and Hrabé de Angelis M. (2006): New ENU induced semidominant mutation, Ali18, causes inflammatory arthri-

tis, dermatitis, and osteoporosis in the mouse. *Mammalian Genome* 17: 915-926.

Chipman SD, Sweet HO, McBride DJ Jr, Davisson MT, Marks SC Jr, Shuldiner AR, Wenstrup RJ, Rowe DW, Shapiro JR. (1993): Defective pro alpha 2(I) collagen synthesis in a recessive mutation in mice: a model of human osteogenesis imperfecta. *Proc Natl Acad Sci USA* 90(5): 1701-5.

Fuchs H, Lisse T, Abe K and Hrabé de Angelis M (2006): Screening for bone and cartilage phenotypes in mice. In: *Phenotyping of the Laboratory Mouse*. Eds.: Hrabé de Angelis M., Chambon P. and Browns S. Wiley-VCH, Weinheim. pp. 35-86.

Fuchs H, Schughart K, Wolf E, Balling R, and Hrabé de Angelis M. (2000): Screening for dysmorphological abnormalities - a powerful tool to isolate new mouse mutants. *Mammalian Genome* 11(7): 528-30.

Gasser JA. (2003): Bone measurements by peripheral quantitative computed tomography in rodents. *Methods Mol Med*. 80:323-41.

Giampietro PF, Blank RD, Raggio CL, Merchant S, Jacobsen FS, Faciszewski T, Shukla SK, Greenlee AR, Reynolds C, Schowalter DB. (2003): Congenital and idiopathic scoliosis: clinical and genetic aspects. *Clin Med Res* 1(2): 125-36.

Hrabé de Angelis, M., H. Flaswinkel, H. Fuchs, B. Rathkolb, D. Soewarto, S. Marschall, S. Heffner, W. Pargent, K. Wuensch, M. Jung, A. Reis, T. Richter, F. Alessandrini, T. Jakob, E. Fuchs, H. Kolb, E. Kremmer, K. Schaeble, B. Rollinski, A. Roscher, C. Peters, T. Meitinger, T. Strom, T. Steckler, F. Holsboer, T. Klopstock, F. Gekeler, C. Schindewolf, T. Jung, K. Avraham, H. Behrendt, J. Ring, A. Zimmer, K. Schughart, K. Pfeffer, E. Wolf and R. Balling (2000): Genome-wide, large-scale production of mutant mice by ENU mutagenesis. *Nature Genetics* 25: 444-447

Mariani FV, Martin GR (2003): Deciphering skeletal patterning: clues from the limb. *Nature* 423(6937): 319-25.

McLean W, Olsen BR. (2001): Mouse models of abnormal skeletal development and homeostasis. *Trends Genet* (10): S38-43.

Rauch F, Glorieux FH. (2004): Osteogenesis imperfecta. *Lancet* 363(9418): 1377-85.

Rosen CJ, Beamer WG, Donahue LR. (2001): Defining the genetics of osteoporosis: using the mouse to understand man. *Osteoporos Int*. 12(10): 803-10.

Schmidt C, Priemel M, Kohler T, Weusten A, Muller R, Amling M, Eckstein F. (2003): Precision and accuracy of peripheral quantitative computed to-

mography (pQCT) in the mouse skeleton compared with histology and microcomputed tomography (microCT). J Bone Miner Res. 18(8):1486-96

Abbreviations

BMC	bone mineral content
BMD	bone mineral density
DXA	dual-energy X-ray absorptiometry
μ CT	micro computed tomography
pQCT	peripheral quantitative computed tomography
pBMD	partial bone mineral density (excluding skull)
sBMD	specific bone mineral density

Table 3: Results from the morphological inspection (10-12-week old mice)				
Parameter	Male		Female	
	Control	Mutant (+/- and -/-)	Control	Mutant (+/- and -/-)
Body appearance				
normal	10	20	10	20
Craniofacial / head morphology				
normal	10	20	10	20
Limbs				
normal	10	20	10	20
Digits				
normal	10	20	10	20
Tail				
normal	10	20	10	20
Eyes				
normal	10	20	10	20
Ears				
normal	10	20	10	20
Teeth				
normal	10	20	10	20
Vibrissae				
normal	10	20	10	20
Coat appearance				
normal	10	20	10	20
Coat / hair growth				
normal	10	20	10	20
Coat / hair texture				
normal	10	20	10	20
Hair follicle structure / orientation				
normal	10	20	10	20
Skin pigmentation				
normal	10	20	10	20
Skin condition / texture				
normal	10	20	10	20
Muscle morphology				
normal	10	20	10	20
Seizures / epilepsy				
no	10	20	10	20
Motor capabilities / coordination				
normal	10	20	10	20
Movement				
normal	10	20	10	20
Eating / drinking behavior				

normal	10	20	10	20
Respiratory system				
normal	10	20	10	20
Reproductive / urinary system				
normal	10	20	10	20
Other abnormalities				
no	10	20	10	20
Animals analyzed	10	20	10	20

Table 4: Results from the X-ray analysis (15-17-week old mice)

Parameter	Male		Female	
	Control	Mutant (+/- and -/-)	Control	Mutant (+/- and -/-)
Skull				
normal	10	20	6	12
Mandibles				
normal	10	20	6	12
Maxilla				
normal	10	20	6	12
Teeth				
normal	10	20	6	12
Orbit				
normal	10	20	6	12
Spine				
normal	10	20	6	12
Number of cervical vertebrae				
normal (7)	10	20	6	12
Number of thoracic vertebrae				
normal (13)	10	20	6	12
Number of lumbar vertebrae				
normal (6)	10	20	6	12
Number of sacral vertebrae				
normal (4)	10	20	6	12
Number of caudal vertebrae				
normal	10	20	6	12
Vertebrae				
normal	10	20	6	12
Ribs				
normal (26)	10	20	6	12
Scapulas				
normal	10	20	6	12
Clavicle				
normal	10	20	6	12
Pelvis				

normal	10	20	6	12
Femur				
normal	10	20	6	12
Tibia				
normal	10	20	6	12
Fibula				
normal	10	20	6	12
Humerus				
normal	10	20	6	12
Ulna				
normal	10	20	6	12
Radius				
normal	10	20	6	12
Digits				
normal (20)	10	19	6	12
left toes crippled (-/-)	-	1	-	-
Joints				
normal	10	20	6	12
Animals analyzed	10	20	6	12

Table 5: Results from clickbox test (hearing test; nine-week old mice)

Phenotype	Male		Female	
	Control	Mutant (+/- and -/-)	Control	Mutant (+/- and -/-)
0	-	-	-	-
1	-	-	-	-
2	-	-	-	-
3	10	20	10	20
4	-	-	-	-
5	-	-	-	-
Mean Score	3.00	3.00	3.00	3.00

Kruskal-Wallis ANOVA on Ranks: n.s.

0: no reaction at all,
1: very slow reaction,
2: retarded reaction,
3: normal reaction,
4: strong reaction,
5: extremely excited

Table 6: Bone- and weight-related quantitative parameters (data presented as mean \pm standard error of mean)												
15-16 - week old mice	HST012 +/+		HST012 +/-		HST012 -/-					ANOVA		
Parameter	Male	Female	Male	Female	Male	Female	+/+ ~ +/-	+/+ ~ -/-	+/- ~ -/-	<i>p</i> – value genotype	<i>p</i> – value sex	<i>p</i> – value interaction
	(n=10)	(n=6)	(n=10)	(n=7)	(n=9)	(n=5)	<i>p</i> – value	<i>p</i> – value	<i>p</i> – value			
BMD [mg/cm ²]	58 \pm 1	61 \pm 2	52 \pm 1	55 \pm 1	51 \pm 2	53 \pm 1	< 0.0001	< 0.0001	n.s.	< 0.0001	< 0.05	n.s.
sBMD [10 ⁻³ x cm ⁻²]	1.79 \pm 0.05	1.86 \pm 0.04	1.78 \pm 0.02	1.92 \pm 0.05	1.86 \pm 0.04	2.11 \pm 0.04	n.s.	< 0.01	< 0.05	< 0.01	< 0.0001	n.s.
BMC [mg]	694 \pm 47	666 \pm 49	555 \pm 45	590 \pm 50	522 \pm 61	474 \pm 39	< 0.05	< 0.01	n.s.	< 0.01	n.s.	n.s.
Bone Content [%]	2.12 \pm 0.12	2.00 \pm 0.06	1.87 \pm 0.11	2.03 \pm 0.10	1.85 \pm 0.14	1.87 \pm 0.10	n.a.	n.a.	n.a.	n.s.	n.s.	n.s.
Body Length [cm]	10.40 \pm 0.07	10.50 \pm 0.00	10.25 \pm 0.08	10.36 \pm 0.09	10.11 \pm 0.11	10.20 \pm 0.12	n.s.	< 0.01	n.s.	< 0.05	n.s.	n.s.
Body Weight [g]	32.60 \pm 0.88	33.23 \pm 1.81	29.40 \pm 0.64	28.79 \pm 1.02	27.79 \pm 1.14	25.22 \pm 0.80	< 0.001	< 0.0001	< 0.05	< 0.0001	n.s.	n.s.
Fat mass [units]	10.84 \pm 1.13	21.55 \pm 2.41	6.23 \pm 0.98	11.40 \pm 2.86	5.75 \pm 1.49	9.86 \pm 4.16	< 0.01	< 0.01	n.s.	< 0.001	< 0.001	n.s.
Fat Content [units x 100/g]	32.79 \pm 2.77	65.86 \pm 7.52	20.75 \pm 2.60	39.38 \pm 9.87	19.85 \pm 4.04	37.76 \pm 15.55	< 0.05	< 0.05	n.s.	< 0.01	= 0.001	n.s.
Lean mass [units]	14.65 \pm 0.76	16.78 \pm 0.98	16.46 \pm 0.56	15.45 \pm 0.87	15.51 \pm 1.05	16.35 \pm 0.83	n.a.	n.a.	n.a.	n.s.	n.s.	n.s.
Lean Content [units x 100/g]	45.37 \pm 2.87	51.73 \pm 5.22	56.44 \pm 2.58	54.21 \pm 3.66	56.60 \pm 4.00	64.88 \pm 2.83	< 0.05	< 0.01	n.s.	< 0.01	n.s.	n.s.

Table 7: Bone-related quantitative parameters (24-26-week old mice): femoral metaphysis (Data presented as mean ± standard error of mean)													
Parameter	HST012 con		HST012 mut -/-		HST012 mut +/-		con ~ mut -/-		con ~ mut +/-		Mut -/- ~ mut +/-		ANOVA
	Male	Female	Male	Female	Male	Female	Male	Female	Male	Female	Male	Female	p – value genotype
	(n=10)	(n=11)	(n=9)	(n=10)	(n=10)	(n=10)	p – value		p – value		p – value		
Total density [mg/cm ³]	636 ± 11	789 ± 6	630 ± 6	793 ± 8	635 ± 5	809 ± 9	n.a.	n.a.	n.a.	n.a.	n.a.	n.a.	n.s.
Trabecular density [mg/cm ³]	307 ± 7	292 ± 6	296↓ ± 5	317↑ ± 3	316 ± 3	304 ± 7	n.a.	<0.001	n.a.	n.a.	<0.05	n.a.	<0.05
Cortical density [mg/cm ³]	818 ± 4	909 ± 6	819 ± 7	888 ± 6	806 ± 4	903 ± 7	n.a.	n.a.	n.a.	n.a.	n.a.	n.a.	n.s.
Total content [mg]	2.16 ± 0.02	2.61 ± 0.03	1.99↓ ± 0.04	2.55↓ ± 0.03	2.15 ± 0.03	2.65 ± 0.03	<0.01	n.s.	n.s.	n.s.	<0.01	<0.05	<0.0001
Trabecular content [mg]	0.37 ± 0.02	0.19 ± 0.01	0.34 ± 0.02	0.17 ± 0.01	0.38 ± 0.01	0.15 ± 0.01	n.a.	n.a.	n.a.	n.a.	n.a.	n.a.	n.s.
Cortical content [mg]	1.79 ± 0.03	2.43 ± 0.03	1.65↓ ± 0.03	2.38↓ ± 0.04	1.77 ± 0.03	2.50 ± 0.03	<0.01	n.s.	n.s.	n.s.	<0.01	<0.05	<0.001
Total area [mm ²]	3.42 ± 0.06	3.32 ± 0.04	3.17 ± 0.08	3.22 ± 0.04	3.39 ± 0.05	3.29 ± 0.06	n.s.	n.s.	n.s.	n.s.	n.s.	n.s.	n.s.
Trabecular area [mm ²]	1.22 ± 0.07	0.65 ± 0.03	1.15 ± 0.05	0.54↓ ± 0.04	1.18 ± 0.04	0.52↓ ± 0.04	n.a.	<0.05	n.a.	<0.05	n.a.	n.a.	<0.05
Cortical area [mm ²]	2.20 ± 0.04	2.67 ± 0.03	2.02↓ ± 0.05	2.68 ± 0.05	2.20 ± 0.04	2.77 ± 0.05	<0.05	n.s.	n.s.	n.s.	<0.01	n.s.	<0.05

Table 8: Bone-related quantitative parameters (24-26-week old mice): femoral diaphysis

(Data presented as mean ± standard error of mean)

Parameter	HST012 con		HST012 mut -/-		HST012 mut +/-		con ~ mut -/-		con ~ mut +/-		Mut -/- ~ mut +/-		ANOVA
	Male	Female	Male	Female	Male	Female	Male	Female	Male	Female	Male	Female	<i>p</i> – value genotype
	(n=10)	(n=11)	(n=9)	(n=10)	(n=10)	(n=10)	<i>p</i> – value		<i>p</i> – value		<i>p</i> – value		
Total density [mg/cm³]	1059 ± 9	1080 ± 8	996↓ ± 9	1067 ± 13	1024↓ ± 11	1090 ± 14	<0.001	n.s.	<0.05	n.s.	n.s.	n.s.	<0.01
Trabecular density [mg/cm³]	231 ± 5	219 ± 5	199↓ ± 6	211 ± 6	220 ± 7	220 ± 15	<0.01	n.s.	n.s.	n.s.	<0.05	n.s.	<0.05
Cortical density [mg/cm³]	1164 ± 7	1182 ± 7	1128↓ ± 3	1169 ± 8	1141↓ ± 8	1177 ± 7	<0.001	n.s.	<0.05	n.s.	n.s.	n.s.	<0.01
Total content [mg]	2.17 ± 0.04	2.12 ± 0.04	1.90↓ ± 0.06	2.03 ± 0.03	2.09 ± 0.04	2.09 ± 0.05	<0.01	n.s.	n.s.	n.s.	<0.05	n.s.	<0.001
Trabecular content [mg]	0.05 ± 0.003	0.05 ± 0.002	0.05 ± 0.005	0.04 ± 0.003	0.06 ± 0.004	0.03 ± 0.005	n.a.	n.a.	n.a.	n.a.	n.a.	n.a.	n.s.
Cortical content [mg]	2.12 ± 0.04	2.07 ± 0.04	1.85↓ ± 0.06	1.98 ± 0.03	2.03 ± 0.03	2.06 ± 0.05	<0.01	n.s.	n.s.	n.s.	<0.05	n.s.	<0.001
Total area [mm²]	2.05 ± 0.04	1.96 ± 0.04	1.92 ± 0.07	1.90 ± 0.03	2.04 ± 0.04	1.92 ± 0.04	n.a.	n.a.	n.a.	n.a.	n.a.	n.a.	n.s.
Trabecular area [mm²]	0.23 ± 0.01	0.21 ± 0.01	0.28 ± 0.03	0.21 ± 0.02	0.26 ± 0.02	0.17 ± 0.03	n.a.	n.a.	n.a.	n.a.	n.a.	n.a.	n.s.
Cortical area [mm²]	1.82 ± 0.03	1.76 ± 0.03	1.64↓ ± 0.05	1.70 ± 0.03	1.78 ± 0.03	1.75 ± 0.05	<0.01	n.s.	n.s.	n.s.	<0.05	n.s.	<0.01

3.2 Behavior Screen

3.2.1 Introduction

Genetic studies in the mouse are important for the elucidation of molecular pathways underlying behavior. The goal of this endeavor is not only the identification of genes that control brain function and influence behavior, but also understanding of genetic factors involved in human psychiatric disorders (Tarrantino & Bucan, 2000; Bucan & Abel, 2002). These disorders are associated with quantitative phenotypes called “intermediate traits” or endophenotypes, some of which, in contrast to the full complex disorder, can readily be modeled in mice. These traits are risk factors which are considered to be closer to the genetic etiology than the full syndrome. Examples are anxiety in depression, prepulse inhibition and working memory deficits in schizophrenia, and social interaction deficits in autism and schizophrenia (Seong *et al.*, 2002; Gottesman & Gould, 2003; Inoue & Lupski, 2003).

In the attempt to efficiently screen for candidate endophenotypes we use Prepulse Inhibition (PPI) to assess sensorimotor gating. PPI is considered to have face, construct, and a high predictive validity for schizophrenia and other neuropsychiatric diseases involving sensorimotor integration dysfunctions in man (Geyer *et al.*, 2001; Swerdlow *et al.*, 1994).

3.2.2 Summary

The behavioural analysis of *HST012* mutants revealed no prepulse inhibition (PPI) sensorimotor differences. This result suggests that the *HST012* mutation does not affect such aspects of central nervous system function.

3.2.3 Mice

Mice were housed with food and water available *ad libitum* under standard laboratory conditions. Animals were separated based on sex, but not genotype. Mice were tested at the age of 11 weeks in PPI. In this screen, 20 female mice (10 control, 10 mutants) and 20 male mice (10 control, 10 mutants) were available for analysis.

3.2.4 Material and Methods

PPI

Prepulse Inhibition (PPI) was assessed using a startle apparatus setup (Med Associates Inc., VT, USA) including 4 identical sound-attenuating cubicles. The protocols were written using the Med Associates “Advanced Startle” software. Experiments were carried out between 08:30h and 17:00h. Background noise was 65 dB, and startle pulses were bursts of white noise (40 msec). A session was initiated with a 5 min acclimation period followed by five presentations of leader startle pulses (110 dB) that were excluded from statistical analysis. Trial types for the PPI included four different prepulse intensities (67, 69, 73, 81 dB); each prepulse preceded the startle pulse (110 dB) by a 50

msec inter-stimulus interval. Each trial type was presented 10 times in random order, organised in 10 blocks, each trial type occurring once per block. Inter-trial intervals varied from 20-30 sec. This protocol is based on the Eumorphia protocol (see www.eumorphia.org), adapted to the specifications of our startle equipment.

Data were statistically analyzed using SPSS software (SPSS Inc, Chicago, USA). The chosen level of significance was $p < 0.05$.

3.2.5 Results

Prepulse Inhibition

Assessment of PPI did not reveal a significant PPI deficit in mutants of both sexes at any prepulse intensity, neither in either sex nor when data of both sexes were pooled (Fig. 3).

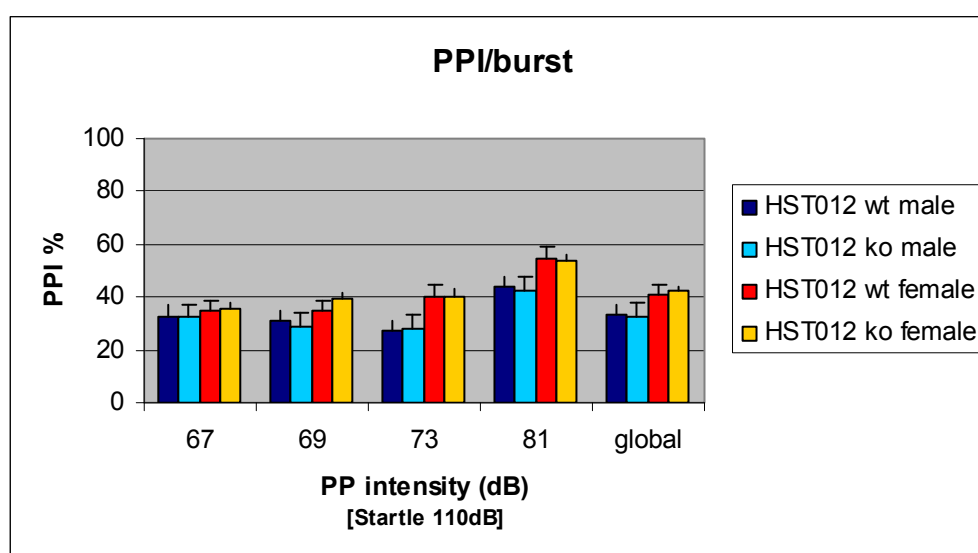


Figure 3: Sensorimotor gating in HST012 mice measured by PPI at a startle intensity of 110 dB and prepulse intensities of 67, 69, 73 and 81 dB. "Global" is the mean PPI value of all four prepulse intensities.

3.2.6 Discussion

The **primary behavioural observation** is that the PPI measurement did not reveal a significant alteration in sensorimotor gating in HST012 mutants. Thus, it would appear that the HST012 mutation does not greatly affect these aspects of central nervous system function.

3.2.7 References

Archer, J. (1973): Tests for emotionality in rats and mice: A review. *Anim. Behav.* 21: 205-235

- Bolivar, V.J., Caldarone, B.J., Reilly, A.A. and Flaherty, L. (2000): Habituation of Activity in an Open Field: A Survey of Inbred Strains and F1 Hybrids. *Behavior Genetics* 30: 285-293.
- Bucan M, Abel T (2002): The mouse: genetics meets behaviour. *Nat Rev Genet* 3: 114-123.
- Choleris E., Thomas AW., Kavaliers M. and Prato F.S. (2001): A detailed ethological analysis of the mouse open field test: effects of diazepam, chlordiazepoxide and an extremely low frequency pulsed magnetic field. *Neurosc. Biobehav. Rev.* 25: 235-260.
- Crawley, J.N. (1989): Animal models of anxiety. *Curr. Opin. Psychiatry* 2: 773-776.
- Geyer MA, Krebs-Thomson K, Braff DL, Swerdlow NR (2001): Pharmacological studies of prepulse inhibition models of sensorimotor gating deficits in schizophrenia: a decade in review. *Psychopharmacol* 156: 117-154.
- Gottesman II, Gould TD (2003): The endophenotype concept in psychiatry: Etymology and strategic intentions. *Am J Psychiatry* 160: 636-645.
- Inoue K, Lupski JR (2003): Genetics and genomics of behavioural and psychiatric disorders. *Curr Opin Genet Dev* 13: 303-309.
- Seong E, Seasholtz AF, Burmeister M (2002): Mouse models of psychiatric disorders. *Trends Genet* 18: 643-650.
- Swerdlow NR, Braff DL, Taaid N, Geyer MA (1994): Assessing the validity of an animal model of deficient sensorimotor gating in schizophrenic patients. *Arch Gen Psych* 51: 139-154.
- Tarantino LM, Bucan M (2000): Dissection of behaviour and psychiatric disorders using the mouse as a model. *Hum Mol Genet* 9: 953-965.
- Weiss SM, Lightowler S, Stanhope KJ, Kennett GA, Dourish CT (2000): Measurement of anxiety in transgenic mice. *Reviews in the Neurosciences* 11: 59-74

3.3 Metabolic Screen

3.3.1 Introduction

The metabolic screening provides a comparative analysis of bioenergetic parameters in mice. Mechanisms which lead to disturbances in body weight regulation and energy metabolism are determined. Hence, the basal energetic demands are monitored during *ad libitum* feeding. In humans, unbalanced energy uptake and energy expenditure cause the development of obesity (Spiegelman and Flier, 2001) or anorexia nervosa with severe weight loss (Hebebrand *et al.*, 2003). The primary metabolic screening focuses on the determination energy expenditure by indirect calorimetry. Body mass, food intake and locomotor activity are monitored under *ad libitum* conditions. These findings serve as the origin for further investigations in secondary and tertiary screening which go into details of energy expenditure and energy storage.

3.3.2 Summary

The primary metabolic screen of homozygous, heterozygous and control HST012 mice revealed several significant differences in energy metabolism parameters. Body mass and body temperature were reduced in mutant mice. Metabolic rate was decreased in mutants as expected for lower body mass but food intake was significantly increased. Interestingly, this was a gradual effect most evident in homozygous mutants. No significant effect of the mutation on metabolic fuel utilization could be detected.

3.3.3 Mice

Ten adult *HST012* wild-type control, 8 heterozygous and 10 homozygous males and entered the Metabolic Screen at the beginning of calendar week 22 in 2008. The females (10 controls, 8 heterozygous and 10 homozygous mice) entered the metabolic laboratory one week later.

3.3.4 Material and Methods

Indirect calorimetry

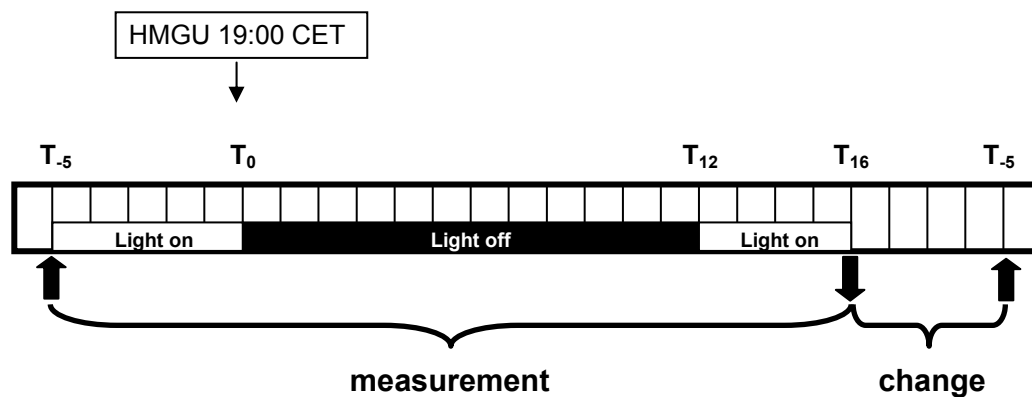
High precision CO₂ and O₂ sensors measure the difference in CO₂ and O₂ concentrations in air volumes flowing through control or animal cages. The amount of oxygen consumed over a given period of time can be calculated with air flow through the cage measured in parallel. Data for oxygen consumption are expressed as ml O₂ h⁻¹animal⁻¹. The system also monitors CO₂ production, therefore, the respiratory exchange ratio (RER) and heat production can be calculated (please see below).

The respiratory exchange ratio (RER) is calculated as the ratio VCO₂/VO₂.

Heat production (HP) is calculated from VO₂ and RER using the formula:

$$\text{HP [mW]} = (4.44 + 1.43 \times \text{RER}) \times \text{VO}_2 [\text{ml h}^{-1}].$$

The test is performed at regular room temperature (23°C) with a 12:12 hrs light/dark cycle in the room (lights on 06:30 CET, lights off 18:30 CET). Paper tissue is provided as bedding material. Each mouse is placed individually in the chamber for a period of about 21 hours (from 14:00 CET to 11:00 CET next day) with free access to food and water. Metabolic chambers are set up in a ventilated cabinet continuously supplied with an overflow of fresh air from outside.



Further data

In addition, body mass before and after the gas exchange measurements are taken. Before returning the mice to their home cage rectal body temperature is also determined. Food intake is monitored by weighing and re-weighing the feeder before and after indirect calorimetry.

Statistical Analysis

All values are presented as means \pm SEM. Two-way-ANOVA (SigmaStat, Jandel Scientific) was used to test for effects of the factors strain and sex (ANCOVA with body mass as covariate). The Fisher test was applied for post hoc multiple comparisons.

3.3.5 Parameters

Recorded and calculated data during metabolic phenotyping
Oxygen consumption (VO_2), Carbondioxide production (VCO_2), Respiratory exchange ratio (RER), heat production (HP), body weight before and after indirect calorimetry, food consumption, and rectal temperature.

3.3.6 Results and Discussion

We detected a stepwise reduction in body mass between heterozygous and homozygous *HST012* mice compared with wild-type control littermates. Body temperature and metabolic rate were also decreased in mutants; both mean

heat production and minimum metabolic rate monitored over 21 hours were lowest in homozygous mutants and intermediate in heterozygous mice. However, food intake (not corrected for spillage) was significantly increased. No significant effect of the mutation on metabolic fuel utilization could be detected.

Prior to the metabolic screening, no effects of the mutation on energy metabolism parameters were reported. The difference in body mass and, possibly, body composition indicated that the mutation affected energy regulation. Even though the difference in metabolic rate can be explained by differences in body composition, increased food intake in mutant mice was noteworthy. It is unclear whether the reduction in body temperature is due to lower metabolic rate or even a compensatory reduction to reduce energetic needs for heat production indicating energy shortage in these mice.

3.3.7 Suggestions for Secondary Screening

Due to the differences in energy metabolism parameters detected in the primary screen we suggest conducting a secondary screen. Firstly, effects of the mutation on food intake and energy assimilation should be confirmed and described in more detail (measuring food intake of single caged mice over several days). During the study body temperature should be monitored. Altogether, the mutation causes a moderate phenotype under *ad libitum* conditions. Therefore, we suggest conducting a fasting test subsequently to evaluate energy regulation in detail.

3.3.8 References

Hebebrand J., C. Exner, K. Hebebrand, C. Holtkamp, R.C. Casper, H. Remschmidt, B. Herpertz-Dahlmann, and M. Klingenspor (2003): Hyperactivity in patients with anorexia nervosa and in semistarved rats: Evidence for a pivotal role of hypoleptinemia. *Physiology and Behavior* 79: 25-37

Spiegelman B.M. and J.S. Flier (2001): Obesity and the regulation of energy balance. *Cell* 104: 531-543

Abbreviations

RER	Respiratory exchange ratio
HP	Heat production
CET	Central European Time

Table 9: Metabolic Parameters Recorded in the Primary Screen									
Data are presented as mean \pm standard error of mean.									
Parameter	<i>HST012 +/+</i>		<i>HST012 +/-</i>		<i>HST012 -/-</i>		2 – Way - ANOVA		
	male (n=10)	female (n=10)	male (n=8)	female (n=8)	male (n=10)	female (n=10)	<i>p</i> <i>genotype</i>	<i>p</i> <i>sex</i>	<i>P</i> <i>interaction</i>
Body weight [g]	31.6 \pm 0.6	28.2 \pm 1.0	29.0 \pm 0.7	24.9 \pm 0.6	26.4 \pm 0.7	24.0 \pm 0.4	<0.001	<0.001	n.s.
Rectal body temperature [°C]	36.62 \pm 0.1	36.99 \pm 0.1	36.11 \pm 0.2	36.63 \pm 0.3	35.57 \pm 0.2	36.31 \pm 0.2	< 0.001	< 0.001	n.s.
Food consumption [g day ⁻¹]	5.1 \pm 0.2	4.9 \pm 0.3	5.4 \pm 0.2	4.6 \pm 0.1	6.1 \pm 0.3	6.0 \pm 0.3	< 0.001	0.05	n.s.
O ₂ consumption, mean [ml h ⁻¹]	100.39 \pm 2.2	102.89 \pm 3.0	93.42 \pm 2.5	92.86 \pm 2.5	85.78 \pm 1.8	89.0 \pm 1.9	<0.001	n.s.	n.s.
RER, mean	0.86 \pm 0.01	0.84 \pm 0.01	0.88 \pm 0.01	0.83 \pm 0.01	0.86 \pm 0.01	0.85 \pm 0.01	n.s.	< 0.001	n.s.
Minimum metabolic rate [mW]	323.1 \pm 11.6	314.1 \pm 18.0	272.9 \pm 7.1	288.2 \pm 6.8	226.7 \pm 7.4	276.2 \pm 7.8	<0.001	<0.05	<0.05
21 hrs heat production [mW]	570.2 \pm 12.8	575.3 \pm 13.6	532.5 \pm 13.2	519.4 \pm 13.6	487.3 \pm 10.4	501.6 \pm 9.7	<0.001	n.s.	n.s.

3.4 Clinical Chemistry and Hematology

3.4.1 Introduction

The aim of the Clinical-Chemical Screen is the detection of hematological changes, defects of various organ systems, and changes in metabolic pathways and electrolyte homeostasis by means of suitable laboratory diagnostic tools. Since most inherited metabolic disorders are known to lead directly or indirectly, via altered organ functions, to changes in the parameters investigated, this screening process provides a comprehensive investigation of clinical phenotypes with counterparts in humans and animal species (Rathkolb *et al.*, 2000). The methods used are routine procedures, allowing the appropriate screen of large numbers of mice for a broad spectrum of clinical-chemical and hematological parameters (Champy *et al.*, 2004; Hough *et al.*, 2002).

3.4.2 Summary

Twenty-one different clinical-chemical plasma parameters were measured including various enzyme activities, as well as plasma concentrations of specific substrates and electrolytes. Additionally, we determined ten basic hematological parameters and blood gas values. Besides the previously known phenotype of impaired kidney function, indicated by increased urea and creatinine values, we detected reduced blood lipid values indicating an influence on energy metabolism, and increased ALP activity and calcium concentrations that might be due to changes in bone metabolism. Blood gas analysis, hematology and iron metabolism-related parameters revealed subtle changes that might be due to secondary effects or simply findings by chance due to biological variation.

3.4.3 Mice

Blood gas values of 10 female mice per genotype aged about 11 weeks were measured in week 19 of 2008. Groups of male mice, also 10 per genotype, were analyzed for blood gas values one week later at the age of about 12 weeks. Blood gas measurement was repeated using a different method of sample collection in week 48 of 2008, using mainly the same mice (some males that were killed for the Molecular Phenotyping Screen had to be substituted) at the age of about 9 months.

In calendar week 24 of 2008, blood samples for clinical chemistry, hematology and other blood based tests were collected from the male mice at the age of 16 to 17 weeks. The female mice were tested one week later. A second sample was collected three weeks after the first one. The mice investigated were kept on an inbred C3HeB/FeJ background.

3.4.4 Materials and Methods

Blood gas analysis

Blood pH, oxygen partial pressure and carbon dioxide partial pressure were measured in capillary blood collected from the retro-orbital sinus of isoflurane-

anesthetized mice using non-heparinized capillaries (1.0 mm in diameter; Neolab; Munich, Germany) and the ABL5 blood gas analyzer (Radiometer GmbH, Willich, Germany). Before sample collection for the first measurement, body temperature of each mouse was measured. Thereafter the mouse was anesthetized, the retroorbital plexus was punctured using the glass capillary, and blood was allowed to drop into a heparin coated sample tube (Li-heparin, KABE; Nümbrecht, Germany; Art.No. 078028) and immediately used to determine temperature corrected blood gas values.

For the second test, body temperature was not determined. This time blood leaking from the glass capillary was directly soaked into an 85µl blood gas capillary (KABE, Nümbrecht, Germany) and immediately used to determine blood gas values at 37°C.

Blood Withdrawal and Storage

For the analysis of blood based parameters blood samples were taken from isoflurane-anesthetized mice by puncturing the retro-orbital sinus with non-heparinized capillaries (1.0 mm in diameter; Neolab; Munich, Germany). The time for sample taking was recorded in a work list. Each blood sample was divided into two portions. The major portion was collected in a heparinized tube (Li-heparin, KABE; Nümbrecht, Germany; Art.No. 078028). The smaller portion was collected (using the same capillary) in an EDTA-coated tube (KABE, Art.No 078035). Each tube was immediately inverted five times to achieve a homogeneous distribution of the anticoagulant.

The Li-heparin-coated tubes were stored in a rack at room temperature for two hours. Afterwards, cells and plasma were separated by a centrifugation step (10 min, 9503 x g; Biofuge, Heraeus; Hanau, Germany). Plasma was distributed between the Immunology Screen (30 µl), the Allergy Screen (30 µl), the Clinical Chemical Screen (130 µl) and the Cardio-Vascular Screen (residual), while the cell pellet was given to the Immunology Screen for FACS-analysis.

The plasma sample for the clinical chemical analysis was transferred into an Eppendorf tube and diluted 1: 2 with aqua dest. The solution was mixed for a few seconds (Vortex genie, Scientific Industries; New York, USA) to prevent clotting and then centrifuged again for 10 min at 9503 x g. In addition, the Clinical Chemical Screen received the EDTA-blood sample for hematological investigations.

Clinical Chemistry

The screen was performed using an Olympus AU 400 autoanalyzer and adapted reagents from Olympus (Hamburg, Germany). Creatinine was measured using a kit from Biomed (Oberschleißheim, Germany). In the primary screen, 21 different parameters were measured including various enzyme activities, as well as plasma concentrations of specific substrates and electrolytes.

Hematology

A volume of 50 µl EDTA-blood was used to measure basic hematological parameters with a blood analyzer, which has been carefully validated for the analysis of mouse blood using the C57BL/6 mouse chip card (ABC-Blutbild-

Analyzer, Scil Animal Care Company GmbH; Viernheim, Germany). Number and size of red blood cells, white blood cells, and platelets are measured by electrical impedance and hemoglobin by spectrophotometry. Mean corpuscular volume (MCV), mean platelet volume (MPV) and red blood cell distribution width (RDW) are calculated directly from the cell volume measurements. The hematocrit (HCT) is assessed by multiplying the MCV with the red blood cell count. Mean corpuscular hemoglobin (MCH) and mean corpuscular hemoglobin concentrations (MCHC) are calculated from hemoglobin/red blood cell count (MCH) and hemoglobin/hematocrit (MCHC), respectively.

Second sample analysis

A second sample was collected from all animals investigated in the first bleeding in order to retest a subset of the parameters measured in the first sample to check the reproducibility of the first results and to provide the steroid screen with plasma samples for their analyses.

Analysis of Data

Data were statistically analyzed using Excel and Sigma Stat 3.1 with the level of significance set at $p < 0.05$, by an ANOVA test on the influence of genotype and sex and subsequent pair-wise comparisons of the means by T-test.

3.4.5 Parameters

Proteins and plasma enzyme activities
Alkaline phosphatase (EC 3.1.3.1), α -Amylase (EC 3.2.1.1), Creatine kinase (EC 2.7.3.2), Aspartate-aminotransferase (ASAT/ GOT; EC 2.6.1.1), Alanine-aminotransferase (ALAT/ GPT; EC 2.6.1.2), Ferritin, Transferrin, Total protein, Albumin
Plasma concentrations of specific substrates
Glucose, Cholesterol, Triglycerides, Urea, Creatinine, Non-esterified fatty acid (NEFA)
Plasma concentrations of electrolytes
Potassium, Sodium, Chloride, Calcium, Inorganic phosphate, Iron
Basic hematology
White blood cell count (WBC), Red blood cell count (RBC) Hematocrit (HCT), Hemoglobin (HGB), Mean corpuscular volume (MCV), Mean corpuscular hemoglobin (MCH), Mean corpuscular hemoglobin concentration (MCHC), Red blood cell distribution width (RDW), Platelet count (PLT) and Mean platelet volume (MPV)
Blood gas analysis
Body temperature, Blood pH, oxygen partial pressure (pO_2), Carbon dioxide partial pressure (pCO_2), Oxygen saturation (sO_2), Bicarbonate concentration (HCO_3^-), Actual base excess (ABE)

3.4.6 Results

Blood gas analysis

In the first test, blood pH and pCO₂ were significantly influenced by the genotype, with the pH being increased and the pCO₂ being reduced in heterozygous as well as homozygous mutant animals compared to the wild-type group (Table 10). However, pO₂ values in general were lower than we usually saw it in capillary blood of C3H mice before, suggesting, that a technical problem might have led to wrong values. Therefore blood gas analysis was repeated using a different method of sample collection in older mice. This time, only the female homozygous mutant mice displayed a slightly higher blood pH (Table 11).

Clinical Chemistry

In the first test, ANOVA revealed a significant influence of the genotype on potassium, calcium, inorganic phosphorus, creatinine, urea, cholesterol, triglyceride, NEFA, and transferrin concentrations as well as ALP activity. Additionally genotype x sex interactions influenced urea and NEFA values. Potassium, creatinine and urea were increased in both, heterozygous and homozygous mutants of both sexes, compared to wild-type controls, while calcium levels were elevated in the homozygous group only. Urea values of homozygous mutant mice were also significantly higher than those of the heterozygous group. Blood lipid values - cholesterol, triglycerides and NEFA – as well as transferrin concentration were significantly decreased in mutant animals, heterozygous as well as wild-type. However, in the case of NEFA in females this was only a tendency. Additionally, ALP activity was significantly increased in homozygous mutants of both sexes (Table 12). In the second test, the measurement of affected parameters was repeated and magnesium and uric acid values were determined additionally. We were able to confirm the findings of increased creatinine and urea concentrations, as well as decreased blood lipid concentrations, although the differences were less strong compared to the first test (Fig. 4). Also the findings of an increased calcium concentration and ALP activity in homozygous mutant mice were confirmed (Fig. 5). Transferrin this time displayed no significant differences, but iron concentration was lower than in controls instead. The increased potassium values in mutants were not confirmed. There was only a tendency in female mutants pointing to the same direction. Magnesium showed no significant influence of the genotype, and for uric acid, only the female homozygous mutant mice displayed significantly higher values than female wild-type mice (Table 4). Interestingly, homozygous and heterozygous males showed very similar values for many parameters, while in the female group heterozygous animals represented an intermediate phenotype (Fig. 4 and 5).

Hematology

In the first test ANOVA revealed a significant influence of the genotype on platelet count (PLT), hemoglobin (HGB), hematocrit (HCT), MCV, MCH and red cell distribution width (RDW). Additionally RDW was influenced by a significant genotype x sex interaction. HGB, HCT and MCV were reduced in both, homozygous and heterozygous mutant animals, with the males being more affected than the females. The male also showed a tendency towards a

reduced red blood cell count. The MCV values of homozygous mutant mice were also significantly lower than those of the heterozygous group. PLT, MCH and RDW were significantly reduced in homozygous mutants and in the case of RDW heterozygous males. For PLT the heterozygous mice showed a tendency to the same direction (Table 13). In the second test, only the findings concerning HGB, HCT and MCV were confirmed (Table 14, Fig. 6).

3.4.7 Discussion

Blood gas analysis

The differences seen in blood gas values were very small, and in the first test possibly false positive due to technical problems. There might be a tendency to develop alkalosis in the mutant animals, but the effect is very small and of unclear relevance. There were clearly no major effects on blood gas values.

Clinical Chemistry

The clinical chemical analyses confirmed the previously known features of increased creatinine and urea levels in homozygous mutant animals and could show that also heterozygous mutants are affected, showing a similar phenotype as the homozygous mice in the male group and an intermediate phenotype in the female group. Additionally we could demonstrate an effect on blood lipid values that were reduced in both heterozygous and homozygous mutant mice. Fitting to this a reduced body weight and an altered body composition were found in the Dymorphology screen, and the results of the Metabolism screen indicated relatively low energy expenditure, if differences in body composition are taken into account. All these findings together indicate an influence of the mutation on energy metabolism even in the heterozygous state. The increased calcium and ALP values in homozygous mutant animals go with the finding of a reduced bone mineral density (BMD) in the Dymorphology screen, indicating, that bone metabolism is affected, probably also even in the heterozygous mice, since the reduction of BMD was also detectable in heterozygous mice. The differences in transferrin and iron were very small and might be findings by chance or could indicate small effects on iron metabolism.

Hematology

Differences detected in the hematological investigation were small and represent most likely secondary effects of uremia – the so called renal anemia – which is due to a reduced life span of erythrocytes and reduced erythropoietin production. However, the differences seen in iron and transferrin could be a hint, that also small changes in iron metabolism might contribute to the changes seen in the peripheral red blood cell count. However, since the differences are very small, these findings are judged to be secondary effects without clinical relevance.

Comparison to baseline data

Sex-related differences were detected for many parameters, reflecting the physiological differences, often observed in various mouse strains (Kile *et al.*, 2003). The clinical-chemical parameters were situated within the normal varia-

tion range of C3H mice as supported by previously published data (Hough *et al.*, 2002; Loeb and Quimby, 1999; Rathkolb *et al.*, 2000; Kile *et al.*, 2003; own unpublished results).

3.4.8 Recommendations for Secondary Screening

We were able to demonstrate an interesting comorbidity affecting kidney function and energy metabolism (food intake, energy assimilation, body temperature and energy regulation) in two mutant mouse lines (HST009 and HST012) with impaired kidney function and the same is already known for the third line HST001. Taken the effects seen in these three lines together, the effect on energy metabolism does not seem to be correlated with the severity of kidney dysfunction, making a secondary effect unlikely. Therefore more detailed investigations on the effects on energy metabolism in collaboration with the Metabolism Screen are recommended. Additionally we suggest to measure the values of energy metabolism related hormones using the Bioplex system trying to clarify the regulatory pathway connecting kidney function and energy metabolism.

3.4.9 References

- Champy, M.-F., M. Selloum, L. Piard, V. Zeitler, C. Caradec, P. Chambon and J. Auwerx (2004): Mouse functional genomics requires standardization of mouse handling and housing conditions. *Mammalian Genome* 15: 768-783
- Hough T.A., P. Nolan, V. Tsipouri, A. Toye, I. Gray, M. Goldsworthy, L. Moir, R. Cox, S. Clements, P. Glenister, J. Wood, R. Selley, M. Strivens, L. Vizer, S. McCormack, J. Peters, E. Fisher, N. Spurr, S. Rastan, J. Martin, S. Brown and A. Hunter (2002): Novel phenotypes identified by plasma biochemical screening in the mouse. *Mammalian Genome* 13: 595-602
- Kile B., C.L. Mason-Garrison and M.J. Justice (2003): Sex and strain-related differences in the peripheral blood cell values of inbred mouse strains *Mammalian Genome* 14: 81 – 85
- Loeb W.F. and Quimby F.W. (1999): *The clinical chemistry of laboratory animals*, Second edition (The Mouse page 3-32) Taylor & Francis, Philadelphia
- Quimby, F. (1999): The Mouse. In: *The clinical chemistry of laboratory animals*, ed. by W. F. Loeb and F. W. Quimby. Taylor and Francis, New York, pp. 3-31
- Rathkolb B., T. Decker, E. Fuchs, D. Soewarto, C. Fella, S. Heffner, W. Pargent, R. Wanke, R. Balling, M. Hrabé de Angelis, H. J. Kolb and E. Wolf (2000): The clinical-chemical screen in the Munich ENU Mouse Mutagenesis Project: screening for clinically relevant phenotypes. *Mammalian Genome* 11: 543-546
- Toye AA, Lippiat J.D., Proks P., Shimomura K., Bentley L., Hugill A., Mijat V., Goldsworthy M., Moir L., Haynes A., Quarterman J., Freemantle HC, Ashcroft FM and Cox RD (2005): A genetic and physiological study of impaired glucose homeostasis in C57BL/6J mice. *Diabetologia* 48(4): 675-86

Table 10: Blood gas analysis, 1 st sample.									
Data are presented as mean ± standard error of mean.									
Group: HST012 Age: 11-12 weeks	Control (A)		Heterozygous (B)		Homozygous (C)		ANOVA		
	male	female	male	female	male	female	genotype	sex	interaction
number of animals tested	10	10	10	10	10	10	<i>p - value</i>	<i>p - value</i>	<i>p - value</i>
Temp (°C) - body	38.12 ± 0.38	37.94 ± 0.17	38.09 ± 0.28	38.1 ± 0.16	37.68 ± 0.24	38.08 ± 0.2	n.s.	n.s.	n.s.
pH	7.31 ± 0.007	7.32 ± 0.005	7.33 ± 0.01	7.34 ± 0.007	7.33 ± 0.007	7.34 ± 0.007	p<0.05	p<0.05	n.s.
pCO2 (mmHg)	48.3 ± 0.94	46.9 ± 1.39	47 ± 1.26	41.6 ± 1.17	44.5 ± 1	42.2 ± 1.23	p<0.01	p<0.01	n.s.
pO2 (mmHg)	44.5 ± 2.73	49 ± 2.02	43.8 ± 2.34	48.9 ± 2.37	42.2 ± 2.59	44.2 ± 2.59	n.s.	p=0.059	n.s.
sO2 (%)	70.7 ± 3.54	77.4 ± 2.44	71.1 ± 2.89	78.3 ± 1.97	70.2 ± 3.5	72.3 ± 3.04	n.s.	p<0.05	n.s.
HCO3- (mmol/l)	23.2 ± 0.49	22.9 ± 0.57	23.4 ± 0.5	21.6 ± 0.56	22.4 ± 0.5	21.8 ± 0.53	n.s.	p<0.05	n.s.
ABE (mmol/l)	-2.7 ± 0.56	-2.6 ± 0.4	-2.1 ± 0.46	-2.9 ± 0.5	-2.7 ± 0.47	-2.9 ± 0.41	n.s.	n.s.	n.s.

Table 11: Blood gas analysis, 2 nd sample.									
Data are presented as mean \pm standard error of mean.									
Group: HST012 Age: 9 months	Control (A)		Heterozygous (B)		Homozygous (C)		ANOVA		
	male	female	male	female	male	female	genotype	sex	interaction
number of animals tested	10	10	10	10	9	10			
Temp ($^{\circ}$ C) analysis	37 \pm 0	37 \pm 0	37 \pm 0	37 \pm 0	37 \pm 0	37 \pm 0	n.a.	n.a.	n.a.
pH	7.33 \pm 0.009	7.31 \pm 0.009	7.34 \pm 0.01	7.31 \pm 0.01	7.33 \pm 0.014	7.35 \pm 0.01	n.s.	n.s.	p<0.05
pCO ₂ (mmHg)	45.5 \pm 1.8	46.3 \pm 1.53	45 \pm 1.06	45.1 \pm 1.51	46.2 \pm 0.95	42.6 \pm 0.78	n.s.	n.s.	n.s.
pO ₂ (mmHg)	63.8 \pm 7.24	57.2 \pm 1.41	56.8 \pm 5.48	51.8 \pm 2.16	48.8 \pm 2.25	51.8 \pm 1.94	n.s.	n.s.	n.s.
sO ₂ (%)	87.4 \pm 1.85	81.4 \pm 5.02	84.1 \pm 2.81	82.3 \pm 2.12	80.1 \pm 2.21	84 \pm 1.69	n.s.	n.s.	n.s.
HCO ₃ ⁻ (mmol/l)	22.3 \pm 1.46	22.5 \pm 0.72	23.5 \pm 0.56	22.2 \pm 0.57	23.89 \pm 0.63	23 \pm 0.47	n.s.	n.s.	n.s.
ABE (mmol/l)	-2.4 \pm 0.52	-3.4 \pm 0.56	-2.1 \pm 0.57	-3.6 \pm 0.58	-1.9 \pm 0.74	-2 \pm 0.56	n.s.	n.s.	n.s.

Table 12: Clinical Chemistry, 1 st sample.									
Data are presented as mean ± standard error of mean.									
Group: HST012 Age 16 weeks	Control (A)		Heterozygous (B)		Homozygous (C)		ANOVA		
	male	female	male	female	male	female	genotype	sex	interaction
number of animals tested	10	10	10	10	10	10	<i>p - value</i>	<i>p - value</i>	<i>p - value</i>
Sodium [mmol/l]	152 ± 1.19	147.8 ± 1.28	152.8 ± 0.68	147.4 ± 0.73	153.8 ± 1.25	147 ± 0.86	n.s.	p<0.001	n.s.
Potassium [mmol/l]	4.34 ± 0.09	4.1 ± 0.06	4.56 ± 0.06	4.44 ± 0.05	4.6 ± 0.13	4.42 ± 0.09	p<0.01	p<0.05	n.s.
Calcium [mmol/l]	2.2 ± 0.02	2.31 ± 0.02	2.19 ± 0.03	2.32 ± 0.02	2.31 ± 0.03	2.35 ± 0.02	p<0.01	p<0.001	n.s.
Chloride [mmol/l]	108.2 ± 1.2	107.8 ± 0.61	109.6 ± 0.64	107.2 ± 0.66	109.7 ± 1.03	106.8 ± 0.7	n.s.	p<0.01	n.s.
inorg. Phosphorus [mmol/l]	1.4 ± 0.09	1.26 ± 0.08	1.08 ± 0.06	1.02 ± 0.1	1.2 ± 0.1	1.1 ± 0.09	p<0.05	n.s.	n.s.
Total Protein [g/dl]	5.28 ± 0.07	5.3 ± 0.09	5.2 ± 0.04	5.18 ± 0.05	5.32 ± 0.12	5.22 ± 0.08	n.s.	n.s.	n.s.
Albumin [g/dl]	2.8 ± 0.042	2.9 ± 0.045	2.782 ± 0.033	2.86 ± 0.031	2.9 ± 0.045	2.88 ± 0.053	n.s.	n.s.	n.s.
Creatinine [mg/dl]	0.142 ± 0.02	0.155 ± 0.01	0.201 ± 0.01	0.213 ± 0.01	0.202 ± 0.02	0.242 ± 0.02	p<0.001	n.s.	n.s.
Urea [mg/dl]	59.5 ± 1.43	60.2 ± 2.95	69 ± 1.41	76.6 ± 2.8	106.8 ± 2.64	94.6 ± 2.76	p<0.001	n.s.	p<0.001
Cholesterol [mg/dl]	155.9 ± 4.67	126.4 ± 4.63	134.6 ± 3.15	112.5 ± 2.69	140.9 ± 4.86	115 ± 3.33	p<0.001	p<0.001	n.s.
Triglycerides [mg/dl]	294 ± 23.8	293 ± 24.3	194 ± 14.7	250 ± 17.9	200 ± 18	192 ± 22.1	p<0.001	n.s.	n.s.

Table 12: Clinical Chemistry, 1st sample.									
Data are presented as mean ± standard error of mean.									
NEFA [mmol/l]	3.62 ± 0.11	1.44 ± 0.06	2.95 ± 0.09	1.28 ± 0.08	3.11 ± 0.16	1.33 ± 0.03	p<0.001	p<0.001	p<0.05
LDH [U/l]	227.4 ± 39.12	230.2 ± 17	250.8 ± 35.11	239.3 ± 11.1	308.5 ± 44.28	215.2 ± 12.91	n.s.	n.s.	n.s.
ALAT [U/l]	20 ± 0.89	22.6 ± 1.46	20.8 ± 3.3	20.8 ± 1.16	28.6 ± 3.88	21 ± 1.87	n.s.	n.s.	n.s.
ASAT [U/l]	42.2 ± 1.94	47.2 ± 3.21	48.8 ± 6.07	49.6 ± 2.98	63.2 ± 9.44	51.2 ± 3.45	p=0.059	n.s.	n.s.
ALP [U/l]	97.4 ± 2.68	118.2 ± 5.21	97.6 ± 3.17	126.4 ± 3.26	115.8 ± 2.72	134.4 ± 5.69	p<0.001	p<0.001	n.s.
α-Amylase [U/l]	613 ± 18.7	532 ± 10.8	600 ± 19.3	527 ± 10.2	599 ± 19.2	557 ± 12.6	n.s.	p<0.001	n.s.
Glucose [mg/dl]	142.6 ± 9	130.9 ± 9.2	144.2 ± 14.1	138.5 ± 5.5	133.6 ± 11.4	144.7 ± 7.2	n.s.	n.s.	n.s.
Ferritin [ng/ml]	26.1 ± 0.96	29.7 ± 1.57	26.8 ± 3.45	29.8 ± 2.81	60 ± 35.44	28.2 ± 3.06	n.s.	n.s.	n.s.
Transferrin [mg/dl]	132.8 ± 1.16	132.8 ± 1.96	128.8 ± 1.03	128.6 ± 1.28	130.7 ± 1.99	127.4 ± 1.03	p<0.05	n.s.	n.s.
Iron [µg/dl]	183.7 ± 7.21	174.8 ± 5.15	180.9 ± 5.29	183.3 ± 10.44	182.1 ± 5.75	158.3 ± 5.88	n.s.	n.s.	n.s.

Table 13: Clinical Chemistry, 2nd sample.

Data are presented as mean ± standard error of mean.

Group: HST012 Age 19 weeks	Control (A)		Heterozygous (B)		Homozygous (C)		ANOVA		
	male	female	male	female	male	female	genotype	sex	interaction
Number of animals tested	6	10	10	10	6	10	<i>p - value</i>	<i>p - value</i>	<i>p - value</i>
Potassium [mmol/l]	4.7 ± 0.1	4.28 ± 0.09	4.68 ± 0.05	4.52 ± 0.11	4.73 ± 0.07	4.48 ± 0.08	n.s.	p<0.001	n.s.
Calcium [mmol/l]	2.31 ± 0.02	2.28 ± 0.02	2.27 ± 0.01	2.32 ± 0.01	2.35 ± 0.02	2.34 ± 0.01	p<0.001	n.s.	p<0.05
Magnesium [mmol/l]	0.78 ± 0.03	0.85 ± 0.02	0.75 ± 0.01	0.87 ± 0.02	0.79 ± 0.02	0.9 ± 0.01	n.s.	p<0.001	n.s.
inorg. Phosphorus [mmol/l]	1.1 ± 0.11	1.22 ± 0.09	0.98 ± 0.07	1.32 ± 0.13	1.03 ± 0.06	1.16 ± 0.09	n.s.	p<0.05	n.s.
Uric Acid [mg/dl]	1.11 ± 0.071	1.56 ± 0.053	1.28 ± 0.236	1.66 ± 0.124	1.13 ± 0.051	1.91 ± 0.103	n.s.	p<0.001	n.s.
Creatinine [mg/dl]	0.176 ± 0.01	0.146 ± 0.02	0.186 ± 0.01	0.186 ± 0.02	0.187 ± 0.01	0.233 ± 0.01	p<0.01	n.s.	p<0.05
Urea [mg/dl]	70.4 ± 5.09	54.7 ± 2.44	70.2 ± 2.2	72.3 ± 1.96	97.7 ± 7.37	91 ± 2	p<0.001	p<0.05	p<0.05
Cholesterol [mg/dl]	176.5 ± 8.4	133.6 ± 3.3	159.4 ± 3.18	128 ± 5.02	167.7 ± 5.37	123.7 ± 2.74	p<0.05	p<0.001	n.s.
Triglycerides [mg/dl]	284 ± 34.6	340 ± 29.2	222 ± 13.7	304 ± 23.4	231 ± 34.8	242 ± 22.8	p<0.05	p<0.05	n.s.
NEFA [mg/dl]	1.92 ± 0.12	1.91 ± 0.08	1.63 ± 0.06	1.72 ± 0.09	1.77 ± 0.13	1.67 ± 0.06	p<0.05	n.s.	n.s.
ALP [U/l]	100.7 ± 3.33	117.8 ± 8	90.4 ± 3.9	128.8 ± 5.68	116 ± 4.59	143.2 ± 6.92	p<0.01	p<0.001	n.s.

Table 13: Clinical Chemistry, 2nd sample.									
Data are presented as mean ± standard error of mean.									
Ferritin [ng/ml]	21.2 ± 4.96	22.8 ± 1.2	18.5 ± 1.74	23.4 ± 2.38	80.9 ± 61.94	24.1 ± 1.31	n.s.	n.s.	n.s.
Transferrin [mg/dl]	136 ± 3.32	135.3 ± 1.71	136.3 ± 2.6	134.5 ± 1.6	133.7 ± 1.94	134.2 ± 1.21	n.s.	n.s.	n.s.
Iron [µg/dl]	209.8 ± 8.08	256.6 ± 12.71	191.5 ± 3.98	221.5 ± 7.68	176.1 ± 4.32	207.5 ± 3.94	p<0.001	p<0.001	n.s.

Table 14: Hematology, 1st sample.

Data are presented as mean ± standard error of mean.

Group HST012 Age 16 weeks	Control (A)		Heterozygous (B)		Homozygous (C)		ANOVA		
	male	female	male	female	male	female	genotype	sex	interaction
number of animals tested	10	10	10	10	10	10	<i>p - value</i>	<i>p - value</i>	<i>p - value</i>
WBC [$10^3/\mu\text{l}$]	6.07 ± 0.39	6.09 ± 0.48	5.97 ± 0.32	5.78 ± 0.39	6.68 ± 0.34	6.46 ± 0.4	n.s.	n.s.	n.s.
RBC [$10^6/\mu\text{l}$]	9.31 ± 0.05	8.59 ± 0.1	9.01 ± 0.09	8.59 ± 0.09	8.99 ± 0.11	8.64 ± 0.1	n.s.	p<0.001	n.s.
PLT [$10^3/\mu\text{l}$]	812 ± 12.8	830 ± 22.6	793 ± 12.3	793 ± 12	732 ± 21.9	780 ± 20.9	p<0.01	n.s.	n.s.
Hemoglobin [g/dl]	14.8 ± 0.09	14.3 ± 0.17	14.1 ± 0.06	14.1 ± 0.15	14 ± 0.1	14.1 ± 0.13	p<0.001	n.s.	p=0.064
Hematocrit [%]	49.5 ± 0.24	45.8 ± 0.57	46.9 ± 0.47	45.2 ± 0.44	46.3 ± 0.49	44.8 ± 0.58	p<0.001	p<0.001	P=0.05
MCV [fl]	53 ± 0.26	53.4 ± 0.27	52.1 ± 0.23	52.7 ± 0.15	51.5 ± 0.31	51.9 ± 0.23	p<0.001	p<0.05	n.s.
MCH [pg]	15.9 ± 0.14	16.7 ± 0.1	15.7 ± 0.1	16.5 ± 0.07	15.5 ± 0.12	16.3 ± 0.11	p<0.01	p<0.001	n.s.
MCHC [g/dl]	29.9 ± 0.18	31.3 ± 0.12	30.2 ± 0.19	31.3 ± 0.11	30.2 ± 0.14	31.5 ± 0.2	n.s.	p<0.001	n.s.
RDW [% of MCV]	13.9 ± 0.08	13.9 ± 0.06	13.5 ± 0.08	13.9 ± 0.15	13.6 ± 0.04	13.5 ± 0.13	p<0.01	n.s.	p<0.05
MPV [fl]	5.59 ± 0.07	5.64 ± 0.08	5.58 ± 0.13	5.52 ± 0.08	5.56 ± 0.12	5.61 ± 0.07	n.s.	n.s.	n.s.

Table 15: Hematology, 2nd sample.

Data are presented as mean ± standard error of mean.

Group HST012 Age 19 weeks	Control (A)		Heterozygous (B)		Homozygous (C)		ANOVA		
	male	female	male	female	male	female	genotype	sex	interaction
number of animals tested	6	10	10	10	6	10	<i>p - value</i>	<i>p - value</i>	<i>p - value</i>
WBC [$10^3/\mu\text{l}$]	6.3 ± 0.48	5.76 ± 0.5	5.64 ± 0.31	5.45 ± 0.35	6.46 ± 0.45	6.21 ± 0.26	n.s.	n.s.	n.s.
RBC [$10^6/\mu\text{l}$]	8.79 ± 0.14	9.03 ± 0.1	8.44 ± 0.07	8.91 ± 0.08	8.56 ± 0.16	8.91 ± 0.1	n.s.	p<0.001	n.s.
PLT [$10^3/\mu\text{l}$]	759 ± 37.4	786 ± 22	797 ± 22.9	769 ± 24.7	726 ± 28.5	734 ± 20.9	n.s.	n.s.	n.s.
Hemoglobin [g/dl]	14.5 ± 0.08	14.8 ± 0.15	14 ± 0.14	14.3 ± 0.09	14.2 ± 0.32	14.3 ± 0.17	p<0.05	n.s.	n.s.
Hematocrit [%]	46.6 ± 0.57	48.2 ± 0.49	44.5 ± 0.5	46.9 ± 0.37	45.3 ± 0.99	46.4 ± 0.57	p<0.01	p<0.001	n.s.
MCV [fl]	53 ± 0.45	53.6 ± 0.27	52.5 ± 0.27	52.6 ± 0.27	52.83 ± 0.48	52.2 ± 0.33	p<0.05	n.s.	n.s.
MCH [pg]	16.6 ± 0.18	16.4 ± 0.11	16.6 ± 0.1	16.1 ± 0.09	16.6 ± 0.18	16 ± 0.16	n.s.	p<0.001	n.s.
MCHC [g/dl]	31.2 ± 0.23	30.6 ± 0.17	31.6 ± 0.12	30.6 ± 0.11	31.3 ± 0.12	30.8 ± 0.19	n.s.	p<0.001	n.s.
RDW [% of MCV]	14.5 ± 0.26	14.5 ± 0.14	14.4 ± 0.13	14.7 ± 0.16	14.5 ± 0.19	14.5 ± 0.16	n.s.	n.s.	n.s.
MPV [fl]	5.61 ± 0.14	5.63 ± 0.09	5.48 ± 0.07	5.64 ± 0.07	5.52 ± 0.18	5.68 ± 0.11	n.s.	n.s.	n.s.

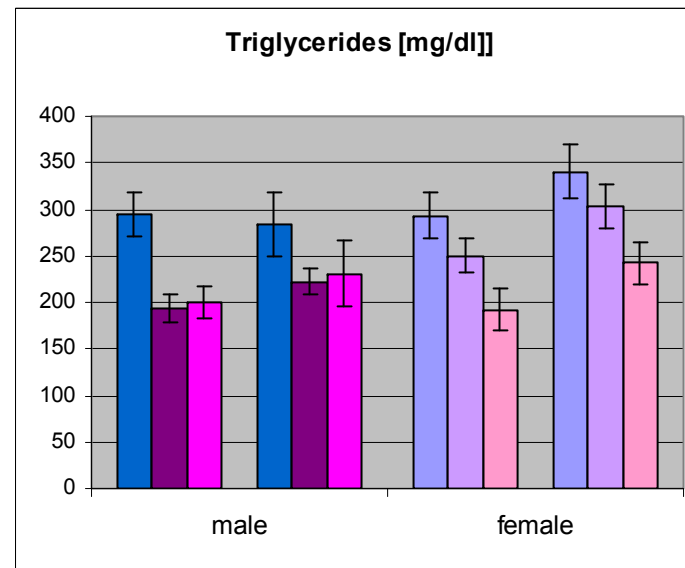
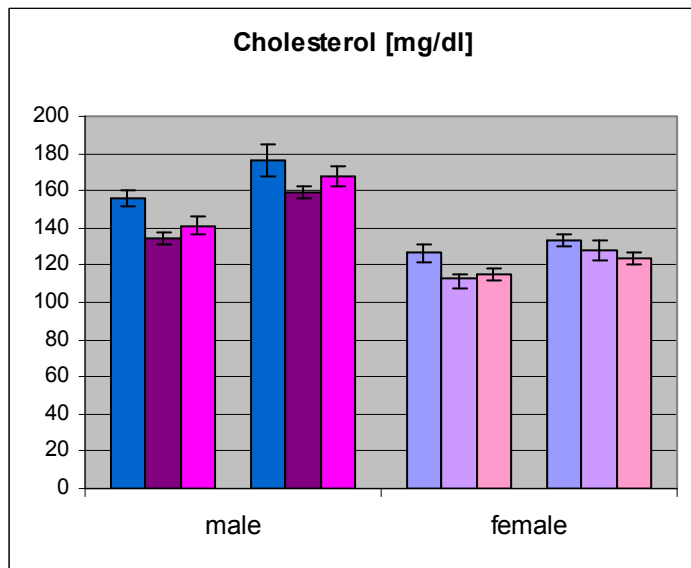
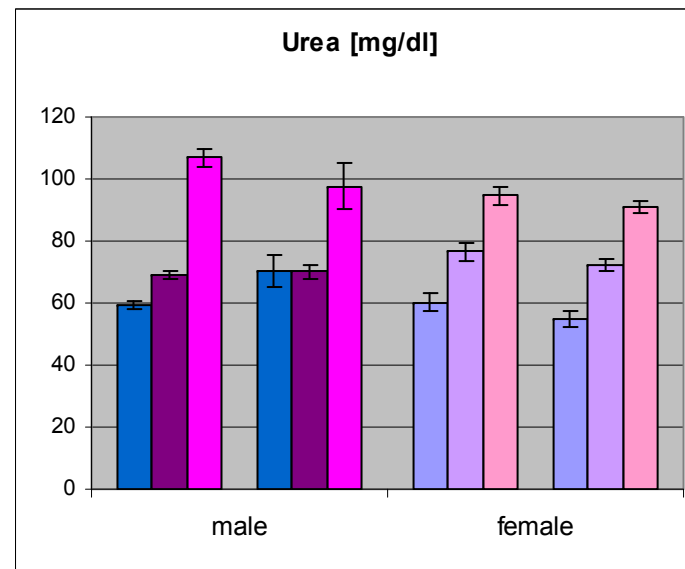
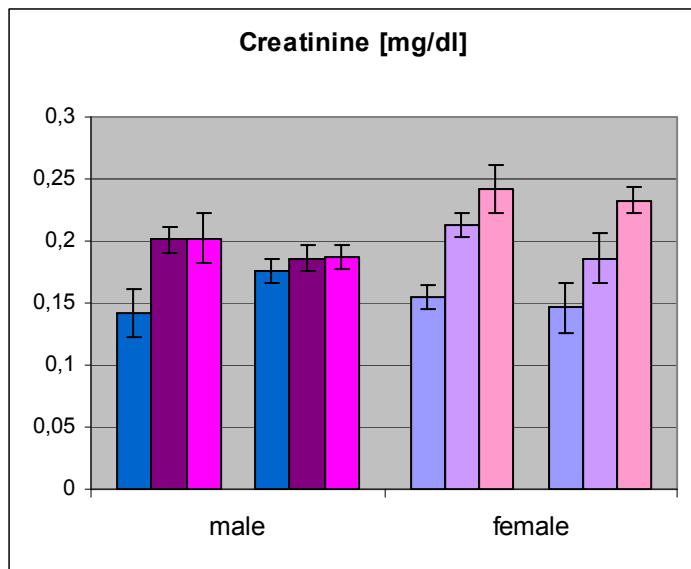


Figure 4: Clinical chemistry of HST012 mice: Creatinine, urea and blood lipid values measured in the first and second samples;

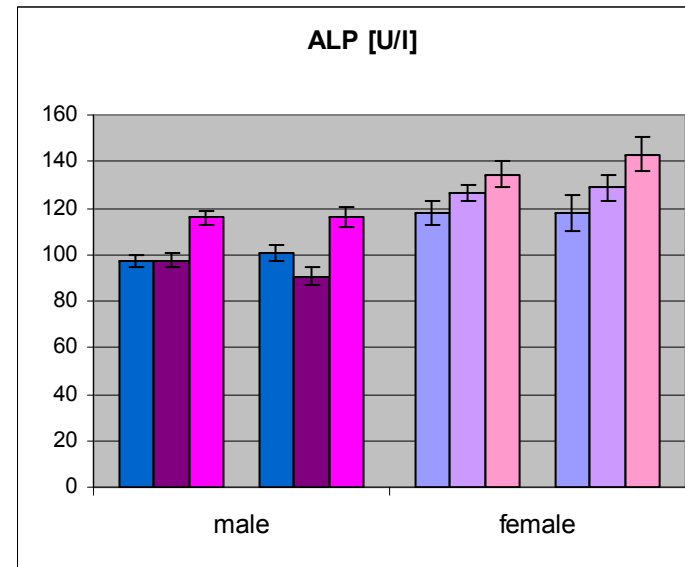
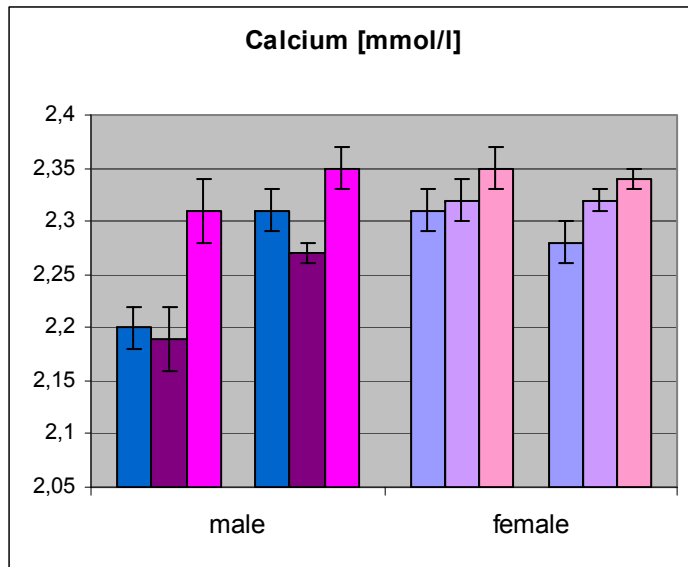


Figure 5: Clinical chemistry of HST012 mice; Calcium concentrations and ALP activities measured in the first and second samples
 WT blue, Heterozygous purple, homozygous pink

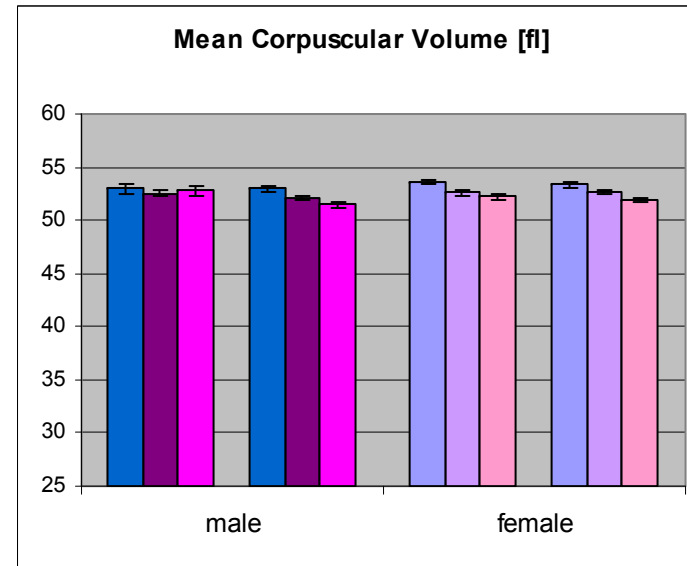
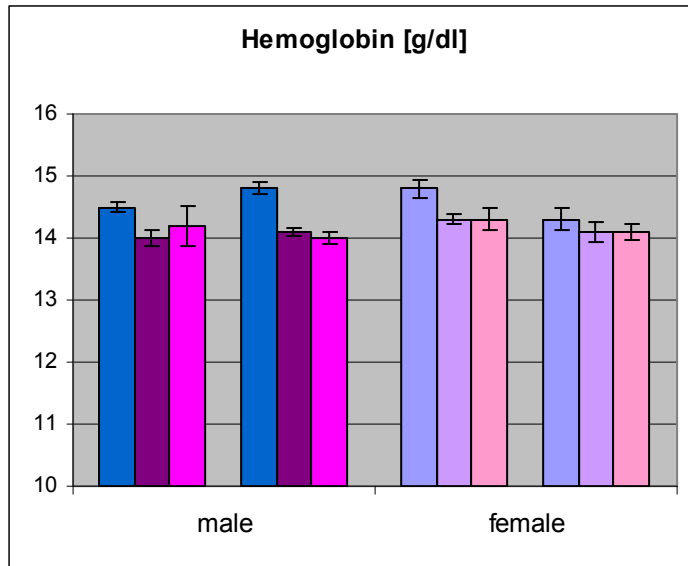


Figure 6: Hematology of HST012 mice; Hemoglobin and MCV measured in the first and second samples

WT blue, Heterozygous purple, homozygous pink

3.5 Immunology Screen

3.5.1 Introduction

Mouse models have been a primary source of information for understanding the intricate mechanisms of the immune system (Blüethmann and Ohashi, 1994; Mak *et al.*, 2001; Fischer 2002; Rogner and Avner, 2003). The Immunology Screen at the GMC was set up to conduct a broad immunological phenotyping of mouse mutant lines with the intention of identifying distinct gene functions, which play key roles in the immune defenses of the organism through a complex network of cellular and soluble components (Janeway *et al.*, 2004). In primary screen we measure leukocyte populations in peripheral blood and immunoglobulin levels in blood plasma.

The proportions of leukocyte populations in peripheral blood are genetically regulated (eg. Mice: Chen and Harrison 2002; Men: Hall, *et al.*, 2000). As a consequence, inbred strains differ in the frequency of leukocyte subsets in the lymphoid organs and in peripheral blood. Moreover, several CD antigens are restricted to specific mouse strains (eg. Carlyle *et al.*, 2006) or interstrain differences occur concerning the level of expression of certain CD antigens (eg. Haegel and Ceredig 2005). Strain specific differences in the immune response are further reflected in different susceptibilities to infectious agents (eg. Medina *et al.*, 2001).

In individual mice, the number of circulating leukocytes and the proportions of subpopulations show daily rhythmic variations (Yellon and Tran 1992) and depend further on homeostatic proliferation and/or retraction (Freitas and Rocha 2000), as well as on activation through environmental and/or microbial factors (eg. Grewal *et al.*, 1997), which might be related to subtle behavioral characteristics (eg. Kim *et al.* 1999). Furthermore, sex-dependent factors are documented to influence the immune status (Krzych *et al.*, 1978) and have an impact on infection susceptibility (Pasche *et al.*, 2005).

The levels of Ig classes and IgG isotypes are characteristic of a special inbred mouse strains and seem to underlie genetic control mechanisms (Sant'Anna *et al.*, 1985).

3.5.2 Summary

A statistically higher expression of CD62L within the CD8 cell cluster occurred in female mutants. In male mutant mice, the proportion of Ly6C expressing cells within the CD8+ T-cell cluster was decreased, in females a higher proportion of Ly6C, CD44 co-expressing CD8 T-cells was found. The analysis of the blood plasma did showed slightly higher levels of IgG2a antibodies in female HST012 mutant mice.

3.5.3 Mice

We analyzed 20 mutant (10 females and 10 males) and twenty (10 females and 10males) of age- and sex-matched littermate controls.

3.5.4 Material and Methods

Peripheral blood leukocytes (PBLs) were isolated from 500 µl blood by erythrocyte lysis with NH₄Cl (0.17M) - Tris buffer (pH 7.45) directly in 96-well mi-

croting plates. After subsequent washing with FACS staining buffer (PBS, 0.5% BSA, 0.02% sodium azide, pH 7.45), PBLs were incubated for 20 min with Fc block (clone 2.4G2, PharMingen, San Diego, USA). Cells were then stained with fluorescence-conjugated monoclonal antibodies (PharMingen). After the antibody incubation, propidium iodide was added for the identification of dying/dead cells (Zamei *et al.*, 1996), which might bind antibodies un-specifically, and/or loose specific antigens upon apoptosis (Diaz *et al.*, 2004). Samples were acquired automatically from 96 well plates with an HTS on a LSRII flow cytometer (Becton Dickinson, USA) until a total number of 30000 living CD45+ cells is reached for each well. For analysis, intact cells are first identified by their FSC/SSC profile. These cells were gated on the basis of their propidium iodide/PE signal (compensated parameters), allowing the dead cells to be gated out. Living cells were then gated using their SSC/CD45 signal, gating out remaining erythrocytes, thrombocytes and debris (Weaver and Broude 2002). CD45+ cells are subsequently analyzed by software based analysis (Flowjo, TreeStar Inc, USA). In former experiments, FMO (Fluorescence minus one) controls from wt mice have been used to define 'positive' and 'negative' regions (Baumgarth and Roederer, 2000).

The plasma levels of IgM, IgG1, IgG2a, IgG2b, IgG3, and IgA were determined simultaneously in the same sample using a bead-based assay (Fulton *et al.*, 1997) with monoclonal anti-mouse antibodies conjugated to beads of different regions (Biorad, USA), and acquired on a Bioplex reader (Biorad). The presence of rheumatoid factor and anti-DNA antibodies was evaluated by indirect ELISA with rabbit IgG (Sigma-Aldrich, Steinheim, Germany) and calf thymus DNA (Sigma-Aldrich), respectively, as antigens and AP-conjugated goat anti-mouse secondary antibody (Sigma-Aldrich). Serum samples from MRL/MpJ-Tnfrsf6lpr mice (Jackson Laboratory, Bar Harbor, USA) were used as positive controls in the autoantibody assays.

3.5.5 Parameters

Flow cytometry
measured parameters and defined cell populations
Main lineages: Staining 1: T-cells (CD3 ⁺), CD4 ⁺ T-cells, CD8 ⁺ T-cells, γ/δ T-cells (CD3 ⁺ γ/δ TCR ⁺), T reg cells (CD4 ⁺ CD25 ⁺), Staining 2: NK cells (NK1.1 ⁺ CD5 ⁻), B-cells (CD19 ⁺), B1 B-cells (CD19 ⁺ CD5 ⁺), mature B-cells (CD19 ⁺ IgD ⁺), granulocytes (CD11b ⁺ Gr1 ⁺⁺),
Subpopulations: Further subpopulations are identified by bi-variate gating with the following markers: Staining 1: CD25, CD62L, Ly-6C, CD44. Staining 2: CD19+ cells: IgD, B220, CD11b, MHC-II(I-A, I-E), CD5, Gr1; CD19- cells: Gr1, B220, CD5, MHCII, CD11b.
Bioplex/ELISA
IgM, IgG ₁ , IgG _{2b} , IgG _{2a} IgG ₃ , IgA; anti-DNA antibodies, rheumatoid factor

3.5.6 Results and Discussion

The analysis of *HST012* mutant mice in the primary Immunology Screen revealed no statistically significant differences in the frequencies of main leukocyte populations between mutant mice compared to controls.

A statistically higher expression of CD62L within the CD8 cell cluster occurred in female mutants. In male mutant mice, the proportion of Ly6C expressing cells within the CD8+ T-cell cluster was decreased (Table 16). These findings occurred also, comparing heterozygous mutant mice with controls. CD62L, L-selectin, is an essential molecule for the homing of naïve T-cells to lymph nodes (Rosen 2004). The higher expression of CD62L on T-cells hints to a more 'naïve' T-cell phenotype, as CD62L mostly gets lost upon activation. In our screening experiences, some variability in the expression of CD62L on T-cells is a frequently occurring phenomenon. High CD62L expression in peripheral blood from humans has been further related to panic disorder (Manfro *et al.* 2000) and nephropathy (De March *et al.* 1999).

Ly6C expression on T-cell has most often been related to memory T-cells or to homeostasis-driven proliferated T-cells, which co-express Ly6C and CD44 (Goldrath *et al.* 2000). *HST012* male mutants did not show a lower proportions of Ly6C and CD44 co-expressing T-cells, however, female mutant mice showed an inverse trend, and a significantly higher proportion of CD44+Ly6C co-expressing CD8 T-cells (Table 17).

Analysis of the plasma immune globulin levels did show slightly higher levels of IgG2a in mutant females compared to controls. However, the relevance of this small difference is unclear. Moreover, we saw very high antibody levels in male mice, both mutants and controls (Table 18).

3.5.7 References

- Baumgarth N and M Roederer (2000): A practical approach to multicolor flow cytometry for immunophenotyping. *J Immunol Methods* 243:77-97.
- Bluethmann H and PS. Ohashi (eds.) (1994): Transgenesis and targeted mutagenesis in immunology. Academic Press, San Diego.
- Carlyle JR, Mesci A, Ljutic B, Belanger S, Tai LH, Rousselle E, Troke AD, Proteau MF, Makrigiannis AP. (2006): Molecular and genetic basis for strain-dependent NK1.1 alloreactivity of mouse NK cells. *J Immunol* 176 (12): 7511-24.
- Chen J and Harrison DE. (2002): Quantitative trait loci regulating relative Lymphocyte proportions in mouse peripheral blood. *Blood* 99(2): 561-566.
- CoutelierJP, Van der Logt JTM, Heessen FWA, Warnier G and Van Snick J. (1987): IgG2a restriction of murine antibodies elicited by viral infections. *J. Exp. Med.* 165: 64.
- De March AK, Bene MC, Renoult E, Kessler M, Faure GC, Kolopp-Sarda MN (1999): Enhanced expression of L-selectin on peripheral blood lymphocytes from patients with IgA nephropathy. *Clin Exp Immunol* 115: 542-546.

- Diaz D, Pietro A, Barcenilla H, Monserrat J, Pietro P, Sánchez MA, Reyes E, Hernandez-Fuentes MP, de la Hera A, Orfao A, Alvarez-Mon M. (2004): Loss of lineage antigens is a common feature of apoptotic lymphocytes. *J Leuk Biol* 76: 609-615.
- Finkelman FD, Katona IM, Mosmann TR and Coffman RL (1988): IFN- γ regulates the isotypes of Ig secreted during in vivo humoral immune responses. *J Immunol.* 140: 1022.
- Fischer A. (2002): Natural mutants of the immune system: a lot to learn! *Eur J Immunol* 32:1519-23.
- Freitas AA, and Rocha B. (2000): Population Biology of Lymphocytes. The Flight for survival. *Annu.Rev.Immunol.*18: 83-11.
- Fulton RJ, McDade R L, Smith PL, Kienker LJ, and Kettman J R, Jr. (1997): Advanced multiplexed analysis with the FlowMetrix system. *Clin Chem* 43:1749-56.
- Grewal IS, Heilig M, Miller A, Sercarz EE. (1997): Environmental regulation of T-cell function in mice: group housing of males affects accessory cell function. *Immunology* 90: 165-168.
- Haegel H and R. Ceredig (1991): Transcripts encoding mouse CD44 (Pgp-1, Ly-24) antigen: strain variation and induction by mitogen. *European Journal of Immunology* 21(6): 1549 – 1553.
- Hermiston ML, Xu Z, Weiss A. (2003): CD45, a critical regulator of signaling thresholds in immune cells. *Annu Rev Immunol.* 21:107-37.
- Janeway C, Travers P, Walport M, Shlomchik M and M.J. Shlomchik (2004): *Immunobiology: The Immune System in Health and Disease*. 6th edition, Garland Publishing, London.
- Manfro GG, Pollack MH, Otto MW, Worthington JJ, Rosenbaum JF, Scott EL, Kradin RL (2000): Cell-surface expression of L-selectin by blood lymphocytes: correlates with affective parameters and severity of panic disorder. *Depression and Anxiety* 11(1):31-37.
- Medina E, Goldmann O, Rohde M, Lengeling A, Chatwals GS. (2001): Genetic control of susceptibility to group A streptococcal infection in mice. *J Infect Dis* 184(7): 846-52. Erratum in: 184(10): 1368.
- Petkova SB, Yuan R, Tsaih SW, Schott W, Roopenian DC, Paigen B (2008): Genetic influence on immune phenotype revealed strain-specific variations in peripheral blood lineages. *Physiol Genomics* 34(3): 304-14.
- Rogner UC and P Avner (2003): Congenic mice: cutting tools for complex immune disorders. *Nat Rev Immunol* 3: 243-252.
- Rubinstein LJ and KE Stein (1988): Murine immune response to the N. meningitid group c capsular polysaccharide: ontogeny. *Jl* 141:4352-4356.
- Sant'Anna OA, Mouton D, Ibanez OM, Bouthillier Y, Mevel JC, Reis MH, Biozzi G. (1985): Basal immunoglobulin serum concentration and isotype distribution in relation to the polygenic control of antibody responsiveness in mice. *Immunogenetics* 22(2):131-9.
- Snapper CM and Paul WE. (1987): Interferon- γ and B-cell stimulatory factor-1 reciprocally regulate Ig isotype production. *Science* 236: 944.
- Stevens TL, Bossie A, Sanders VM, Fernandez-Botran R, Coffman RL, Mosmann TR and Vitetta ES. (1988): Regulation of antibody isotype secretion by subsets of antigen-specific helper T-cells. *Nature* 334: 255.

- Weaver JL and DD Broud (2002): Serial phenotypical analysis of mouse peripheral blood leukocytes. *Toxicology Mechanisms and Methods*, 12: 95-118.
- Yellon SM and LT. Tran (2002): Photoperiod, reproduction, and immunity in select strains of inbred mice. *J Biol Rhythms* 17(1): 65-75.
- Zamai L, Falcieri E, Marhefka G, Viatle M. (1996): Supravital exposure to propidium iodide identifies apoptotic cells in the absence of nucleosomal DNA fragmentation. *Cytometry* 2223: 303-311.

Table 16: Basic parameters analyzed in the Immunology Screen. Flow Cytometry
 Frequencies of main leukocyte subsets in blood of male and female HST012 homozygous mutant and control mice [% of CD45+ viable leukocytes, respectively of parent gate].

Parameter	Control (A)			Mutant -/- (B)			A ~ B	
	Male	Female		Male	Female		Male	Female
	(n=9)	(n=10)	<i>p - value</i>	(n=10)	(n=10)	<i>p - value</i>	<i>p - value</i>	<i>p - value</i>
Tcells(CD3)	27 ± 1.34	37.8 ± 1.15	p<0.001	31.1 ± 1.99	35.9 ± 2.25	n.s.	n.s.	n.s.
8+Tcells	10.17 ± 0.57	13.52 ± 0.41	p<0.001	11.47 ± 0.67	13.36 ± 0.74	n.s.	n.s.	n.s.
4+Tcells	15.23 ± 0.85	21.66 ± 0.69	p<0.001	17.57 ± 1.46	20.59 ± 1.5	n.s.	n.s.	n.s.
gdTcells	0.7 ± 0.07	1.3 ± 0.1	p<0.001	0.9 ± 0.06	1.2 ± 0.08	p<0.01	n.s.	n.s.
4+/Tregs	2.62 ± 0.31	3.17 ± 0.12	n.s.	2.56 ± 0.17	3.15 ± 0.23	n.s.	n.s.	n.s.
4+/44+	48.42 ± 2.11	59.29 ± 0.45	p<0.001	50.96 ± 1.33	58.59 ± 0.62	p<0.001	n.s.	n.s.
4+/62L+	17.836 ± 2.643	12.254 ± 1.955	n.s.	23.77 ± 2.414	18.602 ± 2.54	n.s.	n.s.	n.s.
4+/6C+	2.2 ± 0.27	2.8 ± 0.18	n.s.	2.2 ± 0.2	2.3 ± 0.16	n.s.	n.s.	n.s.
8+/44+	42.88 ± 3.18	53.54 ± 0.62	p<0.01	39.06 ± 4.02	51.9 ± 0.6	p<0.05	n.s.	n.s.
8+/62L+	28.2 ± 2.99	29.5 ± 3.08	n.s.	33.6 ± 1.91	39.8 ± 3.56	n.s.	n.s.	p<0.05
8+/6C+	49 ± 1.2	45 ± 0.9	p<0.05	43 ± 1	43 ± 1.3	n.s.	p<0.01	n.s.
In4-In8	0.4 ± 0.04	0.5 ± 0.02	n.s.	0.4 ± 0.04	0.4 ± 0.03	n.s.	n.s.	n.s.
Bcells	33.9 ± 1.92	21.6 ± 0.93	p<0.001	34.9 ± 2.41	21.4 ± 0.86	p<0.001	n.s.	n.s.
19+/IgD	92.6 ± 0.49	90.6 ± 0.58	p<0.05	93.3 ± 0.35	89.8 ± 0.78	p<0.01	n.s.	n.s.
Granulo-cytes	22.6 ± 2.29	25.5 ± 1.3	n.s.	19.1 ± 2.26	25.7 ± 2.1	p<0.05	n.s.	n.s.
NKTcells	0.46 ± 0	0.7 ± 0	p<0.001	0.46 ± 0	0.73 ± 0	p<0.001	n.s.	n.s.
NK	6.1 ± 0.3	6.5 ± 0.3	n.s.	4.9 ± 0.3	7.2 ± 0.4	p<0.001	p<0.05	n.s.
Monos (CD11b+NK-nonGr)	9.8 ± 0.79	11.7 ± 0.79	n.s.	8.6 ± 0.44	11.2 ± 0.42	p<0.001	n.s.	n.s.

Table 17: Basic parameters analyzed in the Immunology Screen. Flow Cytometry
 Frequencies of main leukocyte subsets in blood of male and female HST012 heterozygous mutant and control mice [% of CD45+ viable leukocytes, respectively of parent gate].

Parameter	Control (A)			Mutant heterozygous (B)			A ~ B	
	Male	Female		Male	Female		Male	Female
	9	10	<i>p</i> - value	10	10	<i>p</i> - value	<i>p</i> - value	<i>p</i> - value
Tcells (CD3)	27 ± 1.34	37.8 ± 1.15	p<0.001	28.3 ± 1.72	36.4 ± 1.08	p<0.01	n.s.	n.s.
8+Tcells	10.17 ± 0.57	13.52 ± 0.41	p<0.001	10.55 ± 0.64	13.31 ± 0.25	p<0.01	n.s.	n.s.
4+Tcells	15.23 ± 0.85	21.66 ± 0.69	p<0.001	15.92 ± 1.27	20.5 ± 0.92	p<0.01	n.s.	n.s.
gdTcells	0.7 ± 0.07	1.3 ± 0.1	p<0.001	0.8 ± 0.07	1.3 ± 0.07	p<0.001	n.s.	n.s.
4+/Tregs	2.62 ± 0.31	3.17 ± 0.12	n.s.	2.84 ± 0.12	3.29 ± 0.2	n.s.	n.s.	n.s.
4+/44+	48.42 ± 2.11	59.29 ± 0.45	p<0.001	50.73 ± 2.06	59.57 ± 0.4	p<0.01	n.s.	n.s.
4+/62L+	17.836 ± 2.643	12.254 ± 1.955	n.s.	21.19 ± 2.102	19.989 ± 2.428	n.s.	n.s.	p<0.05
4+/6C+	2.2 ± 0.27	2.8 ± 0.18	n.s.	2.3 ± 0.28	2.9 ± 0.15	n.s.	n.s.	n.s.
8+/44+	42.88 ± 3.18	53.54 ± 0.62	p<0.01	42.29 ± 3.58	52.15 ± 0.56	p<0.05	n.s.	n.s.
8+/62L+	28.2 ± 2.99	29.5 ± 3.08	n.s.	33.2 ± 3.05	39 ± 2.79	n.s.	n.s.	p<0.05
8+/6C+	49 ± 1.2	45 ± 0.9	p<0.05	44 ± 1.1	40 ± 1.2	p<0.05	p<0.01	p<0.01
In4-In8	0.4 ± 0.04	0.5 ± 0.02	n.s.	0.4 ± 0.03	0.4 ± 0.05	n.s.	n.s.	n.s.
Bcells	33.9 ± 1.92	21.6 ± 0.93	p<0.001	31.8 ± 1.64	21.3 ± 1.41	p<0.001	n.s.	n.s.
19+/IgD	92.6 ± 0.49	90.6 ± 0.58	p<0.05	93.9 ± 0.46	92.1 ± 0.61	p<0.05	n.s.	n.s.
Granulocytes	22.6 ± 2.29	25.5 ± 1.3	n.s.	19.8 ± 2.54	27.4 ± 1.74	p<0.05	n.s.	n.s.
NKTcells	0 ± 0	1 ± 0	p<0.001	0 ± 0	1 ± 0	p<0.001	n.s.	n.s.
NK	6.1 ± 0.3	6.5 ± 0.3	n.s.	6.2 ± 0.5	6.8 ± 0.5	n.s.	n.s.	n.s.
Monos (CD11b+NK-nonGr)	9.8 ± 0.79	11.7 ± 0.79	n.s.	9.4 ± 0.47	11.5 ± 0.64	p<0.05	n.s.	n.s.

Table 18: Basic parameters analyzed in the Immunology Screen. Flow Cytometry
 Frequencies of CD8 T-cell subsets in blood of male and female HST012 mutant and control mice [% of CD8+T-cells, respectively of parent gate].

Parameter	Males			Females			T-Test	
	Control	+/-	-/-	Control	+/-	-/-	Males	Females
	(n=9)	(n=10)	(n=10)	(n=10)	(n=10)	(n=10)	p - value	p - value
8a+3+/Ly6C+	49 ± 1.2	44.1 ± 1.1	43 ± 1.01	39.8 ± 1.22	44.8 ± 0.87	42.5 ± 1.34	Control ~ +/-, -/- p<0.01	Control ~ +/- p<0.01
8a+3+/Ly6C+/CD44+	44.92 ± 3.07	44.7 ± 3.24	41.76 ± 3.77	54.48 ± 0.74	55.62 ± 0.63	53.49 ± 0.5	n.s.	Control ~ -/- p<0.05
8a+3+/Ly6C+/CD44+	21.87 ± 1.31	19.73 ± 1.56	18.11 ± 1.84	21.76 ± 0.89	24.93 ± 0.64	22.78 ± 0.79	n.s.	Control ~ +/-, -/- p<0.05

Table 19: Basic parameters analyzed in the Immunology Screen. Bioplex/ELISA
 Concentration [µg/ml] of antibodies of different isotypes, and levels of autoantibodies (OD) in blood plasma from mutant and controls mice

Parameter	Males			Females			T-Test	
	Control	+/-	-/-	Control	+/-	-/-	Males	Females
	(n=10)	(n=10)	(n=10)	(n=10)	(n=10)	(n=10)	p - value	p - value
IgG1	23889.8 ± 487.11	23844.4 ± 338.75	23884.2 ± 482.23	242.5 ± 23.81	306.7 ± 48.35	227.9 ± 23	n.s.	n.s.
IgG2a	3088.3 ± 122.15	2679.6 ± 226.59	2954.45 ± 193.69	458.32 ± 40.26	554.38 ± 84.59	596.71 ± 46.37	n.s.	control versus -/- p<0.05
IgG2b	4148 ± 458.96	4738.45 ± 428.4	5342.4 ± 627.44	1484.85 ± 182.8	1311.78 ± 92.39	1373.19 ± 225.75	n.s.	n.s.
IgG3	7112.8 ± 172.87	6693.9 ± 432.48	6814.8 ± 181.09	295.9 ± 53.53	382.3 ± 89.78	289.4 ± 61.44	n.s.	n.s.
IgM	7783.85 ± 355.66	8016.95 ± 448.89	7773.6 ± 221.74	813.16 ± 99.8	874.94 ± 99.11	795.35 ± 73.39	n.s.	n.s.
IgA	13007.8 ± 475.63	12889.4 ± 356.2	13099.6 ± 397.35	897.46 ± 73.45	960.98 ± 134	1023.53 ± 102.64	n.s.	n.s.
Anti-DNA	0.673 ± 0.048	0.643 ± 0.06	0.631 ± 0.044	1.217 ± 0.071	1.169 ± 0.044	1.223 ± 0.085	n.s.	n.s.
Rheumatoid factor	0.1 ± 0.02	0.1 ± 0.03	0.1 ± 0.02	0.5 ± 0.04	0.6 ± 0.07	0.5 ± 0.02	n.s.	n.s.

3.6 Allergy Screen

3.6.1 Introduction

The goal of the Allergy screen within the German Mouse Clinic (GMC) is to search for IgE mutants in order to establish mouse models for allergic diseases and to find new strategies for antiallergic therapy. IgE-mediated atopic disorders such as allergic asthma, allergic rhinitis, and atopic dermatitis are now considered as environmentally and exposure driven immune disorders leading to the expression of various clinical phenotypes in individuals with defined genetic risk profiles (Arruda *et al.*, 2005; Kabesch 2006). Genome screens with classical linkage and fine mapping approaches suggest that susceptibility to asthma is determined by multiple genes with each gene having a moderate dose effect (Wjst *et al.*, 1999). In this respect, the development of phenotypically and genotypically defined animal models will be an important step (Bochner and Busse 2005). To detect allergy prone mouse mutants in systematic screening efforts, total plasma IgE was established as a powerful screening parameter (Alessandrini *et al.*, 2001; Jakob *et al.*, 2007).

3.6.2 Summary

The analysis did not reveal any differences in plasma IgE between knockout and control mice.

3.6.3 Mice

An age- and sex-matched group of 20 controls and 20 heterozygous mutant and 19 homozygous mutant animals at the age of 14 weeks were analyzed in the Allergy Screen.

3.6.4 Material and Methods

Fourteen-week-old male and female mice were screened for alterations in plasma total IgE concentrations. Blood samples were taken from animals by puncturing the retroorbital plexus under isoflurane anesthesia.

Plasma was analyzed for total IgE, using a classical immunoassay isotype-specific sandwich ELISA. In brief, microtiter plates (96-well) were coated with 10 µg/ml anti-mouse-IgE rat monoclonal IgG (clone-PC284, The Binding Site) to detect total IgE. Serum samples were diluted 1:10 and standards for murine IgE (Mouse IgE, k clone C38-2 BD Pharmingen™) were appropriately diluted. As secondary antibodies, biotinylated rat anti-mouse IgE (clone R35-118, BD Pharmingen™) were used followed by incubation with BD OptEIA Reagent Set B (Cat. No. 550534 BD Pharmingen™) Plates were analyzed using a standard micro well ELISA reader at 450 nm. Total murine IgE data are reported in ng/ml, based on a standard curve of purified murine IgE (Alessandrini *et al.*, 2001).

3.6.5 Results and Discussion

The analysis of total IgE levels in plasma (Median \pm Stdev) of HST012 mice revealed no statistically significant differences between the groups (Table 20, Fig. 7). In both mutant and control animals, the median concentration of total IgE was higher in females than in males but no significant difference between groups were found. This is a common finding for many mouse inbred strains (Alessandrini *et al.*, 2000; Corteling *et al.*, 2004; Seymour *et al.*, 2002; Melgert *et al.*, 2005).

Taken together, under standard screening conditions for primary Allergy screen, HST012 mice did not show changes in total plasma IgE levels that would reveal a major allergy phenotype.

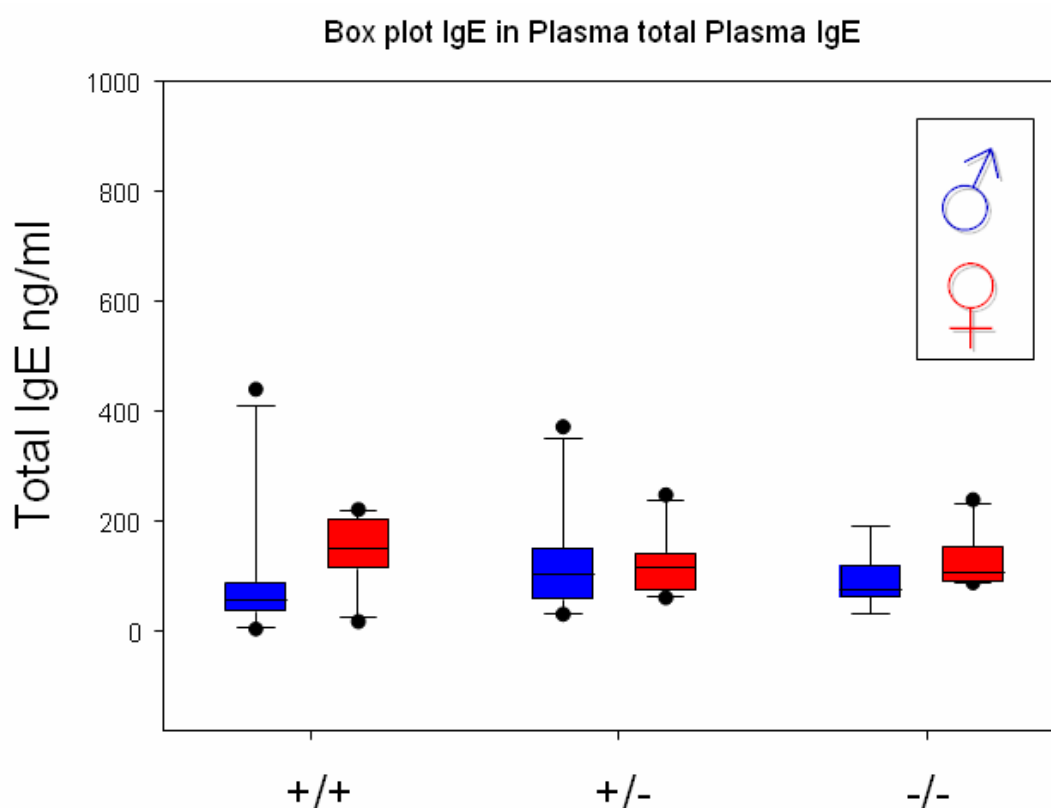


Figure 7: IgE levels in HST012 mice

3.6.6 References

- Alessandrini, F., Jakob, T., Wolf, A., Wolf, E., Balling, R., Hrabé de Angelis, M., Ring, J., and H. Behrendt (2001): ENU mouse mutagenesis: Generation of mouse mutants with aberrant plasma IgE levels. *Int Arch Allergy Immunol* 124: 25-28
- Arruda, L. K., D. Solé, D., Baena-Cagnani, C. E., Naspitz, C. K. (2005): Risk factors for asthma and atopy. *Curr Opin Allergy Clin Immunol* 5(2): 153-9.

- Bochner, B. S. and W. W. Busse (2005): Allergy and asthma. *J Allergy Clin Immunol* 115(5): 953-9.
- Corteling, R. and A. Trifilieff (2004): Gender comparison in a murine model of allergen-driven airway inflammation and the response to budesonide treatment. *BMC Pharmacol* 4: 4.
- Jakob, T., Köllisch GV, Howaldt M, Bewersdorff M, Rathkolb B, Müller ML, Sandholzer N, Nitschke L, Schiemann M, Mempel M, Ollert M, Neubauer A, Soewarto DA, Kremmer E, Ring J, Behrendt H, Flaswinkel H. (2007): Novel mouse mutants with primary cellular immunodeficiencies generated by genome-wide mutagenesis. *J Allergy Clin Immunol*. Sep 2; [Epub ahead of print]
- Kabesch M. (2006): Gene by environment interactions and the development of asthma and allergy. *Toxicol Lett*. 162(1): 43-8.
- Mayuzumi, H., Ohki Y, Tokuyama K, Sato A, Mizuno T, Arakawa H, Mochizuki H, Morikawa A. (2007): Age-related difference in the persistency of allergic airway inflammation and bronchial hyperresponsiveness in a murine model of asthma. *Int Arch Allergy Immunol* 143(4): 255-62.
- Melgert, B. N., Postma DS, Kuipers I, Geerlings M, Luinge MA, van der Strate BW, Kerstjens HA, Timens W, Hylkema MN. (2005): Female mice are more susceptible to the development of allergic airway inflammation than male mice. *Clin Exp Allergy* 35(11): 1496-503.
- Seymour BW, Friebertshauser KE, Peake JL, Pinkerton KE, Coffman RL, Gershwin LJ. (2002): Gender differences in the allergic response of mice neonatally exposed to environmental tobacco smoke. *Dev Immunol*. 9(1): 47-54.
- Shinagawa, K. and M. Kojima (2003): Mouse model of airway remodeling: strain differences. *Am J Respir Crit Care Med* 168(8): 959-67.
- Wjst, M., Fischer G, Immervoll T, Jung M, Saar K, Rueschendorf F, Reis A, Ulbrecht M, Gomolka M, Weiss EH, Jaeger L, Nickel R, Richter K, Kjellman NI, Griese M, von Berg A, Gappa M, Riedel F, Boehle M, van Koningsbruggen S, Schoberth P, Szczepanski R, Dorsch W, Silbermann M, Wichmann HE, et al. (1999): A genome-wide search for linkage to asthma. German Asthma Genetics Group. *Genomics* 58(1): 1-8.

Table 20: Total plasma IgE in HST012 mice

Data are presented as median \pm standard deviation.

Total IgE [ng/ml]	Control (A)			Heterozygous Mice (B)			Homozygous Mice (C)			A~B		A~C		B~C	
	Male	Female	<i>p</i> - value	Male	Female	<i>p</i> - value	Male	Female	<i>p</i> - value	Male	Female	Male	Female	Male	Female
1 st sample	(n=10)	(n=10)	<i>p</i> - value	(n=10)	(n=10)	<i>p</i> - value	(n=9)	(n=10)	<i>p</i> - value	<i>p</i> - value	<i>p</i> - value	<i>p</i> - value	<i>p</i> - value	<i>p</i> - value	<i>p</i> - value
	55.6 \pm 126	151.7 \pm 62	n.s.	102 \pm 98	115 \pm 54	n.s.	76.6 \pm 46	106.5 \pm 48	n.s.	n.s.	n.s.	n.s.	n.s.	n.s.	n.s.

3.7 Steroid Metabolism Screen

3.7.1 Introduction

Steroids control differentiation and proliferation processes of cells and tissues. They participate in the regulation of apoptosis (Bansal *et al.*, 1991), bone remodeling (Jerome, 2004) and neuroregeneration (Chowen *et al.*, 2000). Severe diseases are caused by monogenic mutations with loss of function of steroid pathway proteins. But defects in steroid metabolism contribute as well to the pathogenesis of many different multifactorial diseases like cancer, diseases of cartilage and bone or neurological diseases (Mindnich *et al.*, 2007; Möller *et al.*, 2006; Prehn *et al.*, 2007). The main focus of the Steroid Screen is the identification of new animal models for human steroid-related diseases therewith supporting the development of their future medical treatment. For primary screening the key steroids dehydroepiandrosterone (DHEA) and testosterone (Labrie *et al.*, 1995) are extracted from plasma and quantified by ELISA.

These two steroids were chosen for the tests because of the: 1) robustness of the assay, 2) applicability to mouse model, 3) lack of circadian or other rhythm, 4) indicative value for steroid biosynthesis pathways. Due to low concentrations of plasma steroids, concentration differences can only be considered as significant when they differ in order of magnitude. Generally there are only limited published reference concentrations for the steroids in the rodents. For DHEA in rat was reported to be 1 ng/mL, and for mouse testosterone 5 ng/mL (Kimura *et al.*, 1998, Erben *et al.*, 2002).

3.7.2 Summary

The analysis did not reveal any differences between mutants and control mice.

3.7.3 Mice

Three age- and sex-matched groups of 16 control (6 males, 10 females), 20 heterozygous (10 males, 10 females) and 16 mutant (6 males, 10 females) mice aged 17 weeks have been analyzed in the Steroid Metabolism Screen.

3.7.4 Material and Methods

Male and female mice were screened for alterations in plasma concentrations of DHEA and testosterone. Blood was collected retro-bulbar from 12 weeks old narcotized mice (isoflurane) and plasma was prepared by centrifugation and stored at -20°C.

Since no steroid ELISA kits are available for mouse samples, human ELISA kits have to be used, but analysis is disturbed by the mouse plasma matrix. Therefore, the steroids have to be extracted from the matrix by liquid/liquid-extraction. 40 µl of plasma were extracted three times in each case with 400 µl *tert*-butylmethylether (TBME). The combined organic extracts were evaporated, dissolved *de novo* in TBME, subdivided for the two ELISA tests (15:25 respectively for DHEA and testosterone) and evaporated again.

The material was reconstituted for the respective kit, DHEA in assay puffer, testosterone in steroid free serum.

The steroids are quantified by competitive ELISA according to the manufacturer's protocols. The plates were read in a standard microplate reader at a wavelength of 405 nm (DHEA) and 450 nm (testosterone). The concentrations are reported in pg/ml (DHEA) and ng/ml (testosterone) based on the respective kit standard curve. The sensitivity of the tests is 2.9 pg/ml for DHEA and 0.083 ng/ml for testosterone respectively.

We used the following ELISA kits:

Testosterone ELISA: DRG Instruments GmbH, Catalog No. EIA-1559

DHEA ELISA: AssayDesigns, Catalog No. 901-093

3.7.5 Results and Discussion

At the age of 17 weeks, the analysis of DHEA and testosterone concentrations in plasma *HST012* mice revealed no statistically significant differences between mutants and controls (Table 21/22). In both groups of mutant and control animals, the testosterone levels were significantly higher in males than in females. These are the typical sex-specific differences in the concentration of testosterone.

Table 21: Plasma levels of DHEA and testosterone of <i>HST012</i> mice (17 weeks old)									
Data are presented as median (25 %/75 % - interquartile range)									
	Control (A)			Heterozygous (B)			Mutant (C)		
	Male	Female		Male	Female		Male	Female	
	(n=6)	(n=10)	p - value	(n=10)	(n=10)	p - value	(n=6)	(n=10)	p - value
DHEA [pg/ml]	20.5 (<2.9 / 28.2)	22.7 (7.4 / 49.5)	n.s.	10.8 (<2.9 / 15.0)	17.2 (11.8 / 28.8)	n.s.	19.4 (12.4 / 36.6)	21.7 (10.0 / 64.2)	n.s.
Testosterone [ng/ml]	0.100 (<0.083 / 0.191)	<0.083 (<0.083 / <0.083)	n.s. (0.055)	0.998 (0.193 / 5.095)	<0.083 (<0.083 / <0.083)	0.006	0.342 (<0.083 / 1.326)	<0.083 (<0.083 / <0.083)	0.033

Table 22: Plasma levels of DHEA and testosterone of <i>HST012</i> mice (17 weeks old)						
Data are presented as median (25 %/75 % - interquartile range)						
	Control ~ Hetero		Control ~ Mutant		Hetero ~ Mutant	
	Male P-Value	Female P-Value	Male P-Value	Female P-Value	Male P-Value	Female P-Value
DHEA [pg/ml]	n.s.	n.s.	n.s.	n.s.	n.s.	n.s.
Testosterone [ng/ml]	n.s.	n.s.	n.s.	n.s.	n.s.	n.s.

3.7.6 References

- Bansal N, Houle A and Melnykovich G (1991): Apoptosis: mode of cell death induced in T-cell leukemia lines by dexamethasone and other agents. *Faseb J.* 5: 211-216.
- Chowen JA, Azcoitia I, Cardona-Gomez GP and Garcia-Segura LM (2000): Sex steroids and the brain: lessons from animal studies. *J Pediatr Endocrinol Metab.* 13: 1045-1066.
- Erben RG, Soegiarto DW, Weber K, Zeitz U, Lieberherr M, Gniadecki R, Möller G, Adamski J and Balling R (2002): Deletion of deoxyribonucleic acid binding domain of the vitamin D receptor abrogates genomic and nongenomic functions of vitamin D. *Mol Endocrinol* 16: 1524-1537.
- Jerome CP (2004): Hormonal therapies and osteoporosis. *Ilar J.* 45: 170-178.
- Kimura M, Tanaka S, Yamada Y, Kiuchi Y, Yamakawa T and Sekihara H (1998): Dehydroepiandrosterone decreases serum tumor necrosis factor- α and restores insulin sensitivity: independent effect from secondary weight reduction in genetically obese Zucker fatty rats. *Endocrinology* 139: 3249-3253.
- Labrie F, Belanger A, Simard J, Van L-T and Labrie C (1995): DHEA and peripheral androgen and estrogen formation: intracrinology. *Ann N Y Acad Sci* 774: 16-28.
- Mindnich R, Hrabé de Angelis M and Adamski J (2007): Functional genome analysis indicates loss of 17 β -hydroxysteroid dehydrogenase type 2 enzyme in the zebrafish. *J Steroid Biochem Mol Biol* 103: 35-43.
- Möller, G and Adamski J (2006): Multifunctionality of human 17 β -hydroxysteroid dehydrogenases. *Mol Cell Endocrinol* 248: 47-55.
- Prehn C, Ströhle F, Haller F, Keller B, Hrabé de Angelis M, Adamski J and Mindnich R (2007): A Comparison Of Methods For Assays Of Steroidogenic Enzymes: New GC/MS Versus HPLC And TLC. In: Weiner, H., Plapp, B., Lindhal, R. and Maser, E. (eds.): *Enzymology and Molecular Biology of Carbonyl Metabolism*. Purdue University Press, West Lafayette, Indiana, USA, Vol. 13, pp. 277-283.

3.8 Molecular Phenotyping

3.8.1 Introduction

Comparative genome-wide expression profiling is a powerful tool in the effort to annotate the mouse genome with biological function. The analysis of RNA expression data of mouse lines might support the understanding of the molecular biology of such mutants and provide new insights into mammalian gene function. We demonstrated the feasibility to detect transcriptional affected organs employing RNA expression profiling as a tool for molecular phenotyping (Seltmann *et al.*, 2005). Within the German Mouse Clinic (GMC) we demonstrated the efficiency of systematic genome-wide expression profiling for the detection of molecular phenotypes in organs of a mammalian model organism (Horsch *et al.*, 2008).

3.8.2 Summary

Kidney was chosen for the *HST012* mutant mouse line. In this report, we describe the results of using close to genome-wide 21K cDNA microarrays for the RNA expression profiling of the selected organ of four animals of the *HST012* mutant mouse line. In total 8 chip hybridizations including biological and experimental replicates were performed.

The data analysis and various statistical methods detected several genes differentially regulated between mutant and reference tissue. Several of the significantly regulated genes in kidney are annotated with hemolytic anemia, glomerulosclerosis, hypertension, diabetes and tumorigenesis

3.8.3 Methods and Materials

Organ Collection

The molecular phenotyping screen archives organs of mutant and control mice for subsequent DNA-chip expression profiling analysis. Ten male mice (five mutants and five reference animals) of the *HST012* mutant mouse line were provided to the molecular phenotyping screen.

Organs were collected at the age of 17 weeks. To minimize the influence of circadian rhythm on gene expression, mice were killed between 9 am and 12 am by carbon dioxide asphyxiation. The following 10 organs were collected and archived in liquid nitrogen following our established SOPs (Standard operation protocols): spleen, kidney, testis, liver, heart, lung, thymus, skin/cartilage (outer ear), skeletal muscle and brain. Organs were immediately frozen and stored in liquid nitrogen until isolation of total RNA. The 100 organ samples collected in this collaboration either may be used for further expression profiling analysis in the GMC or alternatively may be transferred to the collaborator.

Isolation of total RNA

Total RNA was isolated just before processing for expression profiling. For preparation of total RNA individual organs were thawed in buffer containing chaotropic salt (RLT buffer, Qiagen) and homogenized using a Polytron ho-

mogenizer. Total RNA from individual samples was obtained according to manufacturer's protocols using RNeasy Midi kits (Qiagen). The concentration was calculated from OD_{260/280} measurement and 2-µg-RNA aliquots were run on a formaldehyde agarose gel to check for RNA integrity. The RNA was stored at -80°C in RNase free water (Qiagen).

Chip Hybridization

Depending on the amount of RNA available for hybridization, in general two chip hybridizations were performed with RNA from all selected organs of each individual mutant mouse. Each chip hybridization was performed against the identical pool of the same organ of reference RNAs (reference RNA pool). For each individual mutant mouse the chip experiments include a color-flip experiment (up to 6 hybridizations/organ).

Reverse Transcription and Fluorescent Labeling

For labeling 15 µg of total RNA were used for reverse transcription and indirectly labeled with Cy3 or Cy5 fluorescent dye according the TIGR protocol (Hegde *et al.*, 2000). Labeled cDNA was dissolved in 50 µl hybridization buffer (6x SSC, 0.5% SDS, 5x Denhardt's solution and 50% formamide) and mixed with 50 µl of reference cDNA solution (pool from six control animals) labeled with the second dye. This hybridization mixture was injected on a pre-hybridized microarray in a HS4800 Hybstation (Tecan) and incubated at 42°C for 16 hours. After hybridization slides were washed with 3x SSC, 1x SSC, 0.5xSSC and 0.1x SSC at room temperature. Slides were dried with nitrogen. Dried slides were scanned with a GenePix 4000A microarray scanner and the images were analyzed using the GenePix Pro6.0 image processing software (Axon Instruments, USA) (Drobyshev *et al.*, 2003; Seltsmann *et al.*, 2005; Greenwood *et al.*, 2005; Mijalski *et al.*, 2005; Horsch *et al.*, 2008).

Significance of Regulation

TIGR software package for Microarray analysis (TM4; Chu *et al.*, 2002, Saeed *et al.*, 2003) was used for normalization (MIDAS: Microarray Data Analysis System; Quackenbush 2002) and identification of genes with significant differential regulation (SAM, Significance Analysis of Microarrays; Tusher *et al.*, 2001). Expression data were normalized performing a total intensity normalization to transform the mean log₂ ratio to zero. To eliminate low-quality array elements several filtering methods were applied. They include: Background checking for both channel with a signal/noise threshold of 2.0, one bad tolerance policy parameter and flip dye consistency checking (Yang *et al.*, 2002).

SAM was used to identify genes with statistically significant changes in expression. Genes were ranked according to their relative difference value d(i), a score assigned to each gene on the basis of change in gene expression levels relative to the standard deviation. Genes with d(i) values greater than a threshold were selected as significantly differentially expressed. The percentage of such genes identified by chance is the false discovery rate (FDR). To estimate the FDR, nonsense genes were identified by calculating permutations of the measurements. The selection of the top differentially expressed genes with reproducible up- or down-regulation includes less than 10% false positives (FDR).

Panther Classification system

The Panther Classification system lists the molecular function, biological process and pathway of each of the regulated gene (Thomas *et al.*, 2003) without any statistical estimation.

BiblioSphere Pathway analysis

To select pathways relevant for the selected genes of an organ we used the BiblioSphere Pathway Edition/Genomatix (Scherf *et al.*, 2005). This software allows a view on our data, integrated in biological networks according to co-citation levels: a) Two genes are co-cited within abstracts, b) two genes are co-cited in one sentence and c) two genes are co-cited restricted to sentences with a function word. In a further analysis significant regulated genes were filtered for two categories of Gene Ontology terms (Biological Processes and Molecular Functions). A GOFilter consists of a hierarchy of terms and the corresponding annotations for the BiblioSphere analysis. A statistical analysis is also performed based on the number of observed and expected annotations of each term. The z-score of the GO-terms indicates whether a certain annotation or group of annotations is over- or underrepresented in a dataset of genes.

3.8.4 Results

Selection of Organs and RNA isolation

Kidney was selected as organ for expression profiling analysis. We isolated total RNA of four mutant mice and four wild type control animals (Table 23).

Table 23: Amount of total RNA [μg] isolated from kidney		
Mouse ID	Genotype	Kidney
30087241	-/-	667
30087252	-/-	594
30087217	-/-	668
30087218	-/-	710
30087242	+/+	807
30087243	+/+	731
30087244	+/+	979
30087245	+/+	720

Chip experiments

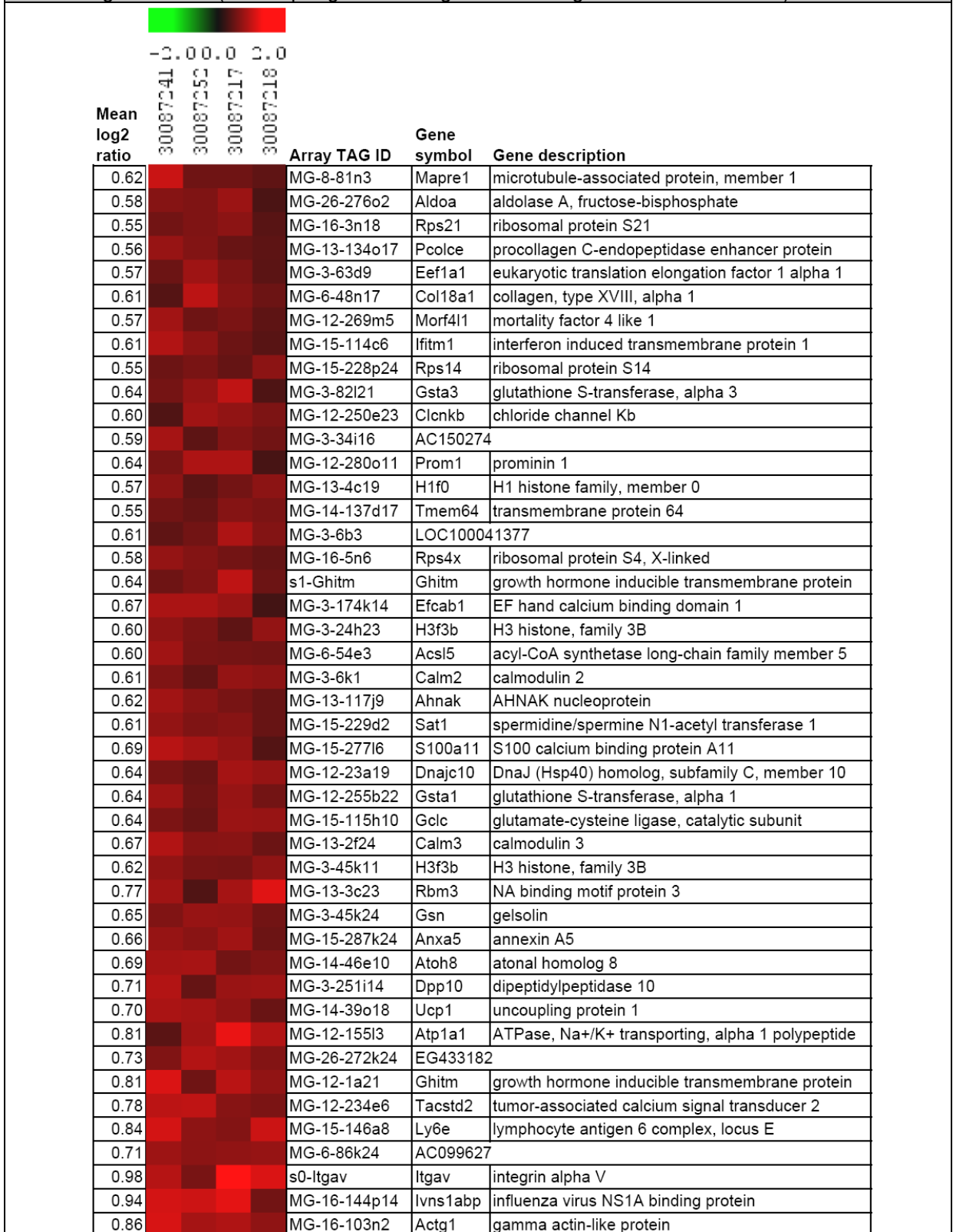
Eight hybridizations were performed for the selected organ.

Gene regulation in Kidney

Table 24 summarizes the results of eight chip hybridisations performed with RNA from kidney. Statistical analysis identified 104 significantly regulated genes. The estimated number of falsely significant genes was calculated for 1000 permutations, yielding a FDR of 0% for this data set including all chip experiments. A FDR of 0% is an indication that all selected genes were reproducibly expressed in all four animals.

Table 24: Heat plots of gene expression profiles from eight DNA microarray experiments of *HST012* mutant versus control mice.

One dye-flip pair represents two experimental replicates of each analyzed animal. One Array TAG ID is the unique probe identifier from the Lion Bioscience clone set. Official gene symbols are given. The scale bar encodes the log ratio of the fold induction; 0% of the elements are above the upper limit of the colour range selection (red is up-regulated and green down-regulation in mutant mice).



0.83		MG-4-3l13	Cd24a	CD24a antigen
0.92		MG-14-22o4	Dgcr2	DiGeorge syndrome critical region gene 2
0.96		MG-12-285g6	Wfdc2	WAP four-disulfide core domain 2
1.05		MG-8-12l22	Serpina1b	serine peptidase inhibitor
1.06		MG-14-3b19	Fabp4	fatty acid binding protein 4
0.96		MG-15-242h2	Cxcl12	chemokine (C-X-C motif) ligand 12
0.86		MG-15-282f8	Abcc4	ATP-binding cassette, sub-family , member 4
1.08		MG-3-7m12	Mt1	metallothionein 1
1.34		MG-14-61c20	Scd1	stearoyl-Coenzyme A desaturase 1
-0.97		MG-6-25l23	AL603662	
-0.92		MG-3-57m19	AC175818	
-0.98		MG-3-237b19	AC147987	
-0.89		MG-3-107a15	BX632059	
-0.91		MG-6-16e20	AL589651	
-0.99		s0-Egr1	Egr1	early growth response 1
-0.95		MG-3-51g19	AC104883	
-0.80		MG-14-64n9	Mark3	MAP/microtubule affinity-regulating kinase 3
-0.74		MG-8-42b9	Hba-a1	hemoglobin alpha, adult chain 1
-0.85		MG-68-104c23	Odc1	ornithine decarboxylase, structural 1
-0.69		MG-3-66c13	Ap2b1	adaptor-related protein complex 2, beta 1 subunit
-0.79		MG-8-86g2	1110017116Rik	
-0.72		MG-8-10b11	Hbb-b1	hemoglobin, beta adult minor chain
-0.79		MG-4-148e12	Hba-a2	hemoglobin alpha, adult chain 2
-0.75		MG-4-86p1	Cpa1	carboxypeptidase A1
-0.75		MG-15-226i17	Uba5	ubiquitin-like modifier activating enzyme 5
-0.74		MG-4-6d16	Tap1	transporter 1, ATP-binding cassette, sub-family B
-0.66		MG-8-42i11	C1qtnf6	C1q and tumor necrosis factor related protein 6
-0.74		MG-12-150l9	Angptl7	angiopoietin-like 7
-0.73		MG-4-3k8	BC056481	
-0.70		MG-3-142i8	9830102E05Rik	
-0.76		MG-4-2e20	Hba-a1	hemoglobin alpha, adult chain 1
-0.66		MG-6-22j19	Fnbp1l	formin binding protein 1-like
-0.69		MG-4-86f7	Hba-a2	hemoglobin alpha, adult chain 2
-0.75		s1-Fbxo32	Fbxo32	F-box protein 32
-0.75		MG-4-147o3	Hba-a1	hemoglobin alpha, adult chain 1
-0.68		MG-26-269p24	Lass1	LAG1 homolog, ceramide synthase 1
-0.84		MG-26-209p19	AC102069	
-0.65		MG-8-71j2	Nup155	nucleoporin 155
-0.69		MG-4-145j12	Hba-a1	hemoglobin alpha, adult chain 1
-0.68		MG-4-148e3	Hba-a2	hemoglobin alpha, adult chain 2
-0.62		MG-3-231k24	LOC100039093	
-0.60		MG-4-5j21	Il6st	interleukin 6 signal transducer
-0.66		MG-16-165f16	Rimbp2	RIMS binding protein 2
-0.57		MG-26-87m22	Rimbp2	RIMS binding protein 2
-1.05		MG-4-3p22	LOC100047628	
-0.62		MG-3-74h9	BX638923	
-0.66		MG-4-3b2	Hba-a1	hemoglobin alpha, adult chain 1
-0.56		MG-12-37p20	Wfdc15b	WAP four-disulfide core domain 15B
-0.59		MG-3-141i13	AL671190	
-0.62		MG-16-193a4	LOC635676	
-0.57		MG-4-4h13	Grp1	glycine/arginine rich protein 1
-0.56		MG-26-144b10	BC024537	

-0.70		MG-15-178d7	CR519226	
-0.57		MG-26-75p13	BC048355	
-0.60		MG-6-42o10	AC122423	
-0.75		MG-6-56d15	Fgf1	fibroblast growth factor 1
-0.58		MG-15-165l2	BC018242	
-0.54		MG-3-171k19	CR516360	
-0.61		s1-Grin2a	Grin2a	glutamate receptor

Classification by molecular functions and biological processes

All significantly regulated genes in kidney were classified (molecular functions and biological processes) using the PANTHER classification system. Additionally, genes were mapped to biological pathways (Table 25).

Table 25: PANTHER classification: kidney			
Gene symbol	Molecular function	Biological processes	Pathway
Actg1	Actin and actin related protein	Exocytosis	
Aldoa	Aldolase	Glycolysis	Fructose galactose metabolism
Anxa5	Transfer/carrier protein	Lipid, fatty acid and steroid metabolism	
Atoh8	Basic helix-loop-helix transcription factor	mRNA transcription regulation	
Atp1a1	Ion channel	Cation transport; Calcium ion homeostasis	
C1qtnf6	Complement component	Complement-mediated immunity	
Calm2	Calmodulin related protein	Calcium mediated signaling; Cell cycle	T-cell and B-cell activation
Calm3	Calmodulin related protein	Calcium mediated signaling; Cell cycle	T-cell and B-cell activation
Cicnkb	Anion channel	Anion transport	
Col18a1	Extracellular matrix structural protein	Angiogenesis	Integrin signalling pathway
Cpa1	Metalloprotease	Proteolysis	
Dpp10	Select regulatory molecule	Cation transport	
Efcab1	G-protein modulator	G-protein mediated signaling	
Egr1	KRAB box transcription factor	mRNA transcription regulation	Angiotensin II-stimulated signaling through G proteins and beta-arrestin
Fabp4	transfer/carrier protein	Lipid and fatty acid transport	
Fbxo32			
Fgf1	Growth factor	Cell surface receptor mediated signal transduction	FGF signaling pathway
Fnbp1l	signaling molecule	Endocytosis	
Gclc	ligase	Sulfur redox metabolism	
Ghitm			
Grin2a	Glutamate receptor	Other receptor mediated signaling pathway	Ionotropic glutamate receptor pathway-
Gsn	Non-motor actin binding protein	Cell structure	FAS signaling pathway
Gsta3	transferase	Detoxification	

H1f0	Histone	Chromatin packaging and remodeling	
H3f3b	Histone	Chromatin packaging and remodeling	
Ifitm1		Cell proliferation and differentiation	
Il6st	Interleukin receptor	Cytokine and chemokine mediated signaling pathway, Hematopoiesis	Interleukin signaling pathway
Itgav	cell adhesion molecule	Cell adhesion	Integrin signalling pathway
Mapre1	Non-motor microtubule binding protein	Cell cycle	
Mark3	Non-motor microtubule binding protein	Protein phosphorylation	
Morf4l1	transcription factor	mRNA transcription regulation	
Nup155	transporter	Nuclear transport	
Pcolce	enzyme regulator	Cell adhesion	
Prom1	Membrane traffic protein	intracellular protein traffic	
Rps14	Ribosomal protein	Protein biosynthesis	
Rps21	Ribosomal protein	Protein biosynthesis	
S100a11	Signaling molecule	DNA replication;DNA replication; Tumor suppressor	
Sat1	transporter	Anion transport	
Scd1	oxidoreductase	Fatty acid metabolism	
Tacstd2	receptor	receptor mediated signaling pathway; Cell proliferation and differentiation	
Tap1	ATP-binding cassette (ABC) transporter	Extracellular transport and import; Immunity and defense	
Ucp1	Mitochondrial carrier protein	Cation transport	
Wfdc2	Serine protease inhibitor	Proteolysis	

In a further analysis significantly regulated genes in kidney were filtered for two categories of Gene Ontology Terms (Molecular and Biological) using the GOFilter Structure of the [BiblioSphere Pathway Edition](#). The z-score of the GO-terms indicates whether a certain annotation or group of annotations is over- or under-represented in the dataset of genes. For genes, differentially expressed in kidney no over-represented GO term for the two categories was identified.

3.8.5 Discussion

Significantly regulated genes could be identified in kidney between mutant and reference tissue.

The function of some of the differentially regulated genes is listed briefly below (Table 26).

Table 26: The function of some of the differentially regulated genes in kidney		
Gene ID	Description	PubMed ID
Abcc4	lipophilic anion transporters, involvement in tumorigenesis	17273943
Acsf5	Involved in different cancer types, role in fatty acid internalization	15900046 15051725
Ahnak	protein marker of endothelial cells, involved in angiogenesis	15493012
Aldoa	Involved in hemolytic anemia	14615364
Anxa5	Involved in tumorigenesis; upregulation is associated with hypertensive heart disease and impairment of systolic function	17988525 17766279
Atoh8	Altered expression in a mouse model of glomerulosclerosis	16937370
Atp1a1	hypertension was associated with the Atp1a1 locus	12884521
Cd24a	expressed on T-cells is essential for homeostatic proliferation	15477346
Clcnkb	implicated in the prevalence of essential hypertension	17997379
Col18a1	inhibits endothelial cell proliferation and migration, as well as tubule formation; increased expression in injured kidney, mainly in the proximal tubule and collecting ducts	17803469
Cxcl12	mediators of leukocyte homeostasis, involved in kidney repair	15840024
Fabp4	Change in expression levels indicate higher cardiovascular disease risk in patients with type 2 diabetes mellitus	18241614
Fbxo32	Involved in cardiac hypertrophy	15489953
Fgf1	Increased expression is associated with hypertension	17909102
Gsta1	cancerogenesis	18414193
Ifitm1	Upregulated in cancer, overexpression negatively regulated cell growth, whereas suppression blocked the antiproliferative effects	17643099 16847454
Il6st	plays an indispensable role in the expansion of hematopoietic precursor cells	12691915
Ly6e	Differentially expressed in irradiated kidney	14680399
Morf4l1	DNA-damage repair in mammalian cells	17961556
Mt1	associated with the incidence of type 2 diabetes	18349110
S100a11	Expressed in renal tumors	15780567
Scd1	Deficient mice had a reduced level of liver triglyceride and an improvement in insulin sensitivity, important role in regulating lipid metabolism and cell function in renal proximal straight tubules	17605312 16368743
Ucp1	higher expression of uncoupling protein might prevent mitochondria-mediated neuronal injury and, ultimately, diabetic neuropathy	16373902
Wfdc15b	constitutively expressed in kidney and epididymis	12574366

The differential expression of *Ghitm*, *H3f3b*, *Hba-a1*, *Hba-a2* and *Rimbp2* in kidney was confirmed by up to five independent probes on the array. These different probes for the identical gene show similar regulation. The fact, that independent probes for the same gene show similar expression levels give additional confidence in these expression profiling data.

Conclusion

Using the statistical methods described above, a number of genes that are differentially expressed in kidney of *HST012* mutant mice were identified. The relevance of these genes in terms of the studied allele should be evaluated. Please, contact us if you have questions concerning this analysis.

3.8.6 References

- Beckers, J., Herrmann, F., Rieger, S., Drobyshev, A., Horsch, M., Hrabé de Angelis, M. and Seliger, B. (2005): Identification and validation of novel *ERBB2* (*Her2*, *NEU*) targets including genes involved in angiogenesis. *Int. J. Cancer* 114: 590-597.
- Drobyshev, A.L., Machka, C., Horsch, M., Seltmann, M., Liebscher, V., Hrabé de Angelis, M. and Beckers, J. (2003): Specific assessment from fractionation experiments (SAFE): a novel method to evaluate microarray probe specificity based on hybridization stringencies. *Nucl. Acids Res.*, 31, E1-1.
- Frey, I.M., Rubio-Aliaga, I., Siewert, A., Sailer, D, Drobyshev, A., Beckers, J., Hrabé de Angelis, M., Aubert, J., Bar Hen, A., Fiehn, O., Eichinger, H.M., and Daniel, H. (2007). Profiling at mRNA, protein and metabolite level reveals alterations in renal amino acid handling and glutathione metabolism in kidney tissue of *Pept2*^{-/-} mice. *Physiol Genomics* 28:301-310.
- Greenwood AD, Horsch M, Stengel A, Vorberg I, Lutzny G, Maas E, Schädler S, Erfle V, Beckers J, Schätzl H and Leib-Mösch C (2005): Cell Line Dependent RNA Expression Profiles of Prion-infected Mouse Neuronal Cells. *JMB* 349: 487-500
- Hegde P, Qi R, Abernathy R, Gay C, Dharap S, et al (2000): A concise guide to cDNA microarray analysis-II. *Biotechniques* 29: 548-56
- Quackenbush J (2002): Microarray data normalization and transformation. *Nature Genetics* 32: 496-501
- Saeed AI, Sharov V, White J, Li J, Lioang W, Bhagabati N, Braisted J, Klapa M, Currier T, Thiagarajan M, Sturn A, Snuffin M, Rezantsev A, Popov D, Ryltsov A, Kostukovich E, Borisovsky I, Liu Z, Vinsavich A, Trush V, Quackenbush J (2003): TM⁴: a free, open-source system for microarray data management and analysis. *Biotechniques* 34 (2):374-8
- Scherf M, Epple A and Werner T (2005): The next generation of literature analysis: integration of genomic analysis into text mining. *Brief Bioinform* 6(3):287-97
- Seltmann, M., Horsch, M., Drobyshev, A., Chen, Y., Hrabé de Angelis, M. and Beckers, J. (2005): Assessment of a Systematic Expression Profiling Approach in ENU-Induced Mouse Mutant Lines. *Mamm. Genome*, 16, 1-10.
- Tusher VG, Tibshirani R and Chu G (2001): Significance analysis of microarrays applied to the ionizing radiation response: *Proceedings of the National Academy of Sciences USA* 98: 5116-5121
- Yang YH, Dudoit S, Luu P, Lin DM, Peng V, Ngai J and Speed TP (2002): Normalization for cDNA microarray data: a robust composite method addressing single and multiple slide systematic variation. *Nuc Acid Research* 30(4): e15

Acknowledgements

A large team consisting of scientists, technicians and animal caretakers all contribute to the success of the German Mouse Clinic. We want to thank Reinhard Seeliger, Elfi Holupirek, Susanne Axtner, Miriam Backs, Christine Fürmann, Tamara Halex, Sabine Holthaus, Nadine Kink, Claudia Kloss, Regina Kneuttinger, Kerstin Kutzner, Maria Kugler, Jacqueline Müller, Elenore Samson, Sandra Schädler, Ann-Elisabeth Schwarz, Bettina Sperling, Susanne Wittich, and Claudia Zeller for expert technical help and Daniela Kißling, Manuela Huber, Petra Thalmeier, Sabine Schwarz, and Anica Miedl for the care of the mice.

Appendix: Tables

Table 1: HST012 mice provided for analysis.	4
Table 2: Primary Screen at GMC	9
Table 3: Results from the morphological inspection (10-12-week old mice)	16
Table 4: Results from the X-ray analysis (15-17-week old mice)	17
Table 5: Results from clickbox test (hearing test; nine-week old mice).....	18
Table 6: Bone- and weight-related quantitative parameters.....	19
Table 7: Bone-related quantitative parameters (24-26-week old mice): femoral metaphysis	20
Table 8: Bone-related quantitative parameters (24-26-week old mice): femoral diaphysis	21
Table 9: Metabolic Parameters Recorded in the Primary Screen	28
Table 10: Blood gas analysis, 1 st sample.....	35
Table 11: Blood gas analysis, 2 nd sample.....	36
Table 12: Clinical Chemistry, 1 st sample.....	37
Table 13: Clinical Chemistry, 2 nd sample.....	39
Table 14: Hematology, 1 st sample.....	41
Table 15: Hematology, 2 nd sample.....	42
Table 16: Basic parameters analyzed in the Immunology Screen. Flow Cytometry	51
Table 17: Basic parameters analyzed in the Immunology Screen. Flow Cytometry	52
Table 18: Basic parameters analyzed in the Immunology Screen. Flow Cytometry	53
Table 19: Basic parameters analyzed in the Immunology Screen. Bioplex/ELISA .	53
Table 20: Total plasma IgE in HST012 mice.....	57
Table 21: Plasma levels of DHEA and testosterone of <i>HST012</i> mice (17 weeks old)	59
Table 22: Plasma levels of DHEA and testosterone of <i>HST012</i> mice (17 weeks old)	59
Table 23: Amount of total RNA [µg] isolated from kidney.....	63
Table 24: Heat plots of gene expression profiles from eight DNA microarray experiments of <i>HST012</i> mutant versus control mice.....	64
Table 25: PANTHER classification: kidney	66
Table 26: The function of some of the differentially regulated genes in kidney ...	68

Figures

Figure 1: Workflow of the primary screen.....	5
Figure 2: pQCT scout view and CT scan of the femur.	12
Figure 3: Sensorimotor gating in HST012 mice measured by PPI at a startle intensity of 110 dB and prepulse intensities of 67, 69, 73 and 81 dB. “Global” is the mean PPI value of all four prepulse intensities.	23
Figure 4: Clinical chemistry of HST012 mice: Creatinine, urea and blood lipid values measured in the first and second samples;.....	43
Figure 5: Clinical chemistry of HST012 mice; Calcium concentrations and ALP activities measured in the first and second samples	44
Figure 6: Hematology of HST012 mice; Hemoglobin and MCV measured in the first and second samples	45
Figure 7: IgE levels in HST012 mice	55

Addresses of screeners and modules

Coordinators

Dr. Valérie Gailus-Durner
Dr. Helmut Fuchs
Barbara Ferwagner
Dr. Christoph Lengger
Dr. Beatrix Naton
Prof. Dr. Martin Hrabé de Angelis
Institute of Experimental Genetics
Helmholtz Zentrum München
German Research Center for Environ-
mental Health (GmbH)
Ingolstädter Landstraße 1
D-85764 Neuherberg
Tel.: 089-3187-3613
Fax: 089-3187-3500
Email: gailus@helmholtz-muenchen.de

Behavior Screen

Dr. Sabine M. Hölter
Dr. Lillian Garrett
Institute of Developmental Genetics
Helmholtz Zentrum München
German Research Center for Environ-
mental Health (GmbH)
Ingolstädter Landstraße 1
D-85764 Neuherberg
Tel.: 089-3187-3674
Fax: 089-3187-3099
Email: hoelter@helmholtz-muenchen.de

Dysmorphology Screen,

Dr. Helmut Fuchs
Dr. Wolfgang Hans
Prof. Dr. Martin Hrabé de Angelis
Institute of Experimental Genetics
Helmholtz Zentrum München
German Research Center for Environ-
mental Health (GmbH)
Ingolstädter Landstraße 1
D-85764 Neuherberg
Tel.: 089-3187-3151
Fax: 089-3187-3500
Email: hfuchs@helmholtz-muenchen.de

Neurology Screen

Dr. Lore Becker
Eva Kling
German Mouse Clinic (GMC)/Neurology
Institute of Experimental Genetics
Helmholtz Zentrum München
German Research Center for Environ-
mental Health (GmbH)
Ingolstädter Landstraße 1
D-85764 Neuherberg
Tel.: 089-3187-3654
Fax: 089-3187-3500
Email: [lore.becker@helmholtz-
muenchen.de](mailto:lore.becker@helmholtz-muenchen.de)

PD Dr. Thomas Klopstock
Friedrich-Baur-Institut,
Neurologische Klinik
Ludwig-Maximilians-Universität München
Ziemssenstraße 1a
D-80336 München
Tel: 089-5160-7474
FAX: 089-5160-7402
Email: [Thomas.Klopstock@med.uni-
muenchen.de](mailto:Thomas.Klopstock@med.uni-muenchen.de)

Eye Screen

Dr. Claudia Dalke
Dr. Oliver Puk
Institute of Developmental Genetics
Helmholtz Zentrum München
German Research Center for Environ-
mental Health (GmbH)
Ingolstädter Landstraße 1
D-85764 Neuherberg
Tel.: 089-3187-2910
Fax: 089-3187-2210
Email: [oliver.puk@helmholtz-
muenchen.de](mailto:oliver.puk@helmholtz-muenchen.de)

Clinical-Chemical Screen

Dr. Birgit Rathkolb
GMC - German Mouse Clinic
Clinical-Chemical Screen
Institute of Experimental Genetics
Helmholtz Zentrum München
German Research Center for Environ-
mental Health (GmbH)
Ingolstädter Landstraße 1
D-85764 Neuherberg
Tel.: 089-3187-3282
Email: [birgit.rathkolb@helmholtz-
muenchen.de](mailto:birgit.rathkolb@helmholtz-muenchen.de)

Prof. Dr. Eckhard Wolf
Institute of Molecular Animal Breeding
and Biotechnology
Genecenter
LMU München
Feodor Lynen-Straße 25
D-81377 München
Tel.: 089-21807-6800
Email: ewolf@lmb.uni-muenchen.de

Immunology Screen

Dr. Thure Adler
Prof. Dr. Dirk Busch
GMC - German Mouse Clinic
Institute for Experimental Genetics
Helmholtz Zentrum München
German Research Center for Environmental Health (GmbH)
Ingolstädter Landstraße 1
D-85764 Neuherberg
Tel.: 089-3187-3656
Fax: 089-3187-3500
Email: thure.adler@helmholtz-muenchen.de

Prof. Dr. Dirk Busch
Institute for Medical Microbiology,
Immunology and Hygiene
Technische Universität München (TUM)
Trogerstr. 9
D-81675 München
Tel.: 089-4140-6191
Fax: 089-4140-4139
Email: dirk.busch@lrz.tum.de

Allergy Screen

Anahita Javaheri, MSc
Antonio Aguilar
Prof. Dr. Markus Ollert
Klinik und Poliklinik für Dermatologie
und Allergologie am Biederstein
Technische Universität München (TUM)
Biedersteinerstraße 29
D-80802 München
Tel.: 089-4140-3551 (M.O.)
Tel.: 089-3187-2554 (A.J.)
Fax: 089-4140-3552
Email: ollert@lrz.tum.de

Steroid Screen

Dr. Cornelia Prehn
Prof. Dr. Jurek Adamski
Institute of Experimental Genetics
Helmholtz Zentrum München
German Research Center for Environmental Health (GmbH)
Ingolstädter Landstraße 1
D-85764 Neuherberg
Tel.: 089-3187-3231
Fax: 089-3187-3500
Email: prehn@helmholtz-muenchen.de

Nociceptive Screen

Dr. Ildikó Rácz
Laboratory of Molecular Neurobiology
Department of Psychiatry
University of Bonn
Sigmund-Freud-Straße 25
D-53105 Bonn
Tel.: 0228-688-5316
Fax: 0228-688-5301
Email: iracz@uni-bonn.de

Prof. Dr. Andreas Zimmer
Laboratory of Molecular Neurobiology
Department of Psychiatry
University of Bonn
Sigmund-Freud-Straße 25
D-53105 Bonn. Germany
Tel.: 0228-688-5303

Lung Function Screen

Dr. Ines Bolle
Prof. Dr. Holger Schulz
Institute for Inhalation Biology
Helmholtz Zentrum München
German Research Center for Environmental Health (GmbH)
Ingolstädter Landstraße 1
D-85764 Neuherberg
Tel.: 089-3187-4119
Fax.: 089-3187-2400
Email: schulz@helmholtz-muenchen.de

Molecular Phenotyping

Dr. Marion Horsch
Dr. Johannes Beckers
Institute of Experimental Genetics
Helmholtz Zentrum München
German Research Center for Environmental Health (GmbH)
Ingolstädter Landstraße 1
D-85764 Neuherberg
Tel.: 089-3187-3513
Fax: 089-3187-4085
Email: horsch@helmholtz-muenchen.de

Metabolic Screen

Dr. Jan Rozman
Nicole Ehrhardt
Institute of Experimental Genetics
GMC - German Mouse Clinic
Metabolic Screen
Helmholtz Zentrum München
German Research Center for Environmental Health (GmbH)
Ingolstädter Landstraße 1
D-85764 Neuherberg
Tel.: 089-3187-3807
Fax: 089-3187-3500
Email: jan.rozman@helmholtz-muenchen.de

Prof. Dr. Martin Klingenspor
Technische Universität München
Nutrition and Food Research Center
Molecular Nutrition
Am Forum 5
D-85350 Freising-Weihenstephan

Cardiovascular Screen

Dr. Anja Schrewe
Institute of Experimental Genetics
GMC - German Mouse Clinic
Cardiovascular Screen
Helmholtz Zentrum München
German Research Center for Environmental Health (GmbH)
Ingolstädter Landstraße 1
D-85764 Neuherberg
Tel.: 089-3187-3646
Fax: 089-3187-3500
Email: anja.schrewe@helmholtz-muenchen.de

Dr. Boris Ivandic
Prof. Dr. Hugo Katus
Innere Medizin III
Otto-Meyerhof-Zentrum
Im Neuenheimer Feld 350
D-69120 Heidelberg
Tel.: 06221 - 56-1505
Email: boris_ivandic@med.uni-heidelberg.de

Pathology Screen

Dr. Julia Calzada-Wack
Dr. Gabriele Hölzlwimmer
Dr. Ilona Moßbrugger
PD Dr. Irene Esposito
PD Dr. Leticia Quintanilla-Martinez
Institute of Pathology
Helmholtz Zentrum München
German Research Center for Environmental Health (GmbH)
Ingolstädter Landstraße 1
D-85764 Neuherberg
Tel.: 089-3187-3241
Fax: 089-3187-3360
Email: irene.esposito@helmholtz-muenchen.de